# Free surface flow due to a submerged source

Student: Holger Paul Keeler, BSc, BTech

Supervisor: Dr Scott McCue

Faculty of Science

Griffith University

arXiv:1402.4002v1 [physics.flu-dyn] 17 Feb 2014

Submitted in partial fulfillment of the requirements of

the degree of Bachelor of Science with Honours

October 27, 2005

# Abstract

In fluid mechanics a free surface problem entails a free moving interface between one fluid (usually water) and another fluid (usually air). Due to the unknown form of the interface and the nonlinear boundary conditions applied there, free surface problems are highly nonlinear and almost impossible to solve analytically.

In this project we consider the free surface flow due to a submerged source in a channel of finite depth. This problem has been considered previously in the literature, with some disagreement about whether or not a train of waves exist on the free surface for Froude numbers less than unity. The physical assumptions behind the accepted model are clearly stated and governing equations and boundary conditions derived. Complex variable theory is then employed to obtain a singular nonlinear integral equation, which describes the flow field completely.

The integral equation is evaluated numerically using a collocation method, and implemented with mathematical software *Matlab*. The numerical solutions suggest that indeed waves do exist on the free surface, but are exponentially small in the limit that the Froude number approaches zero. An asymptotic expression is also derived to solve the integral equation, valid for small Froude numbers. This expansion is calculated to second order, which improves on the leading order solution given previously in the literature. Such a scheme is unable to predict waves on the free surface, since they are exponentially small. It is discussed how exponential asymptotics could be used to derive a more accurate analytic solution that describes waves on the free surface.

This work has not previously been submitted for a degree or diploma in any university. To the best of my knowledge and belief, the dissertation contains no material previously published or written by another person except where due reference is made in the dissertation itself.

_____

Holger Paul Keeler

# Contents


**1 Introduction** **1**

1.1 Flow problems with free-surfaces . . . . . 1

1.2 Flow due to a submerged source or sink . . . . . 2

1.3 Goals of this project . . . . . 4

**2 Mathematical Formulation** **6**

2.1 Physical assumptions . . . . . 6

2.2 Problem description . . . . . 7

2.3 Governing equations . . . . . 8

2.4 Kinematic conditions . . . . . 9

2.5 Dynamic conditions . . . . . 9

2.6 Nondimensionalizing . . . . . 10

2.7 Froude numbers . . . . . 11

2.8 Summary . . . . . 12

**3 Boundary Integral Method** **13**

3.1 Complex variables . . . . . 13

3.2 Symmetry of the system . . . . . 14

3.3 Potential function . . . . . 15

3.4 Mapping the potential . . . . . 16

3.5 Logarithmic hodograph . . . . . 17

3.6 Boundary values . . . . . 18

3.7 Cauchy's Theorem . . . . . 18

3.8 Mapping back to the physical plane . . . . . 21

3.9 Bernoulli's Equation on the $\zeta$-plane . . . 22
3.10 Nonlinear integral equation . . . 22

**4 Numerical Scheme** **24**
4.1 System equations . . . 24
4.2 Singularities . . . 26
4.3 Equation solving scheme . . . 27
4.4 Summary . . . 28

**5 Asymptotic Analysis** **30**
5.1 Upstream height for a solution with no waves . . . 30
5.2 Regular perturbation method for $F_{SP} \ll 1$ . . . 31
5.3 Asymptotic description which includes waves . . . 34

**6 Presentation of Results** **36**
6.1 Effects of numerical scheme parameters . . . 36
6.2 Comparison of numerical and asymptotic solutions . . . 38
6.3 Wave behaviour . . . 40

**7 Conclusion and Discussion** **44**
7.1 Summary of project . . . 44
7.2 Related free surface problems . . . 45
7.2.1 Flow past the stern of a ship . . . 45
7.2.2 Flow under a sluice gate . . . 47
7.3 Further research . . . 48
7.3.1 Exponential Asymptotics . . . 48
7.3.2 Flow due to a sink . . . 48
7.3.3 Stern flows . . . 49

**A Numerical code** **50**
A.1 *froudesolve.m* . . . 50
A.2 *froude.m* . . . 52
A.3 *trapezoid.m* . . . 54

# List of Figures


2.1 2-D profile of stagnation point with submerged source. . . . . 7
2.2 Profile of the free surface problem with nondimensional variables. . . . . 11

3.1 Right-hand side of problem with a solid boundary located to the left. . . . . 15
3.2 The problem on the $f$-plane. . . . . 16
3.3 The problem mapped to the lower half of the $\zeta$-plane. . . . . 17
3.4 The semi-circle $\Gamma$ separated into different regions on the $\zeta$-plane. . . . . 19

6.1 A comparison of free surface profiles to observe the effect of different approximations for infinity. $F_{SP} = 0.4$. . . . . 37
6.2 The effect on the numerical solution when the number of mesh points is varied. $F_{SP} = 0.4$, $F_B = 0.4677$ and $\mu = 0.9009$. . . . . 38
6.3 Comparison of asymptotic and numerical free surface profiles for $F_{SP} = 0.2$. . 39
6.4 Comparison of asymptotic and numerical $\delta$ solutions for $F_{SP} = 0.2$. . . . . 39
6.5 The asymptotic solutions breaks down for $F_{SP} = 0.45$. . . . . 40
6.6 Asymptotic solution is unable to predict waves for $F_{SP} = 0.45$ . . . . . 41
6.7 A linear fit of the numerical results that suggest $A$ decreases exponentially. . 41
6.8 A fitted line with an almost unity gradient suggesting an exact expression for $k$. 42
6.9 Narrower crests and broader troughs for $F_{SP} = 0.5$. . . . . 43
6.10 The free surface angle, $\delta$ becoming skewed for $F_{SP} = 0.5$. . . . . 43

7.1 Flow past a regular ship stern. . . . . 45
7.2 Flow past a rectangular ship stern. . . . . 46
7.3 The lower half of the $\zeta$-plane. . . . . 47
7.4 Flow under a sluice gate with two free surfaces. . . . . 48

# Chapter 1

# Introduction

Historically, the behaviour of fluids, particularly water, has been an extensively studied area in engineering, physics and applied mathematics. For the simplest problems, much light has been shed on this field over the years. However, when treating more detailed and interesting cases the governing equations and boundary conditions become increasingly complex and nonlinear. Depending on their complexity and nature, fluid mechanic problems can be divided into different classes and various analytical and numerical solutions are developed accordingly. In this thesis we investigate one interesting class of problems known as free surface problems, which are highly nonlinear in nature, and must be treated with a combination of analytical and numerical means. In particular, we shall consider a steady state flow system due to a source or sink submerged in a channel of fluid.

## 1.1 Flow problems with free-surfaces

The class of problems where the uppermost surface is the interface between one fluid (usually water) and another fluid (usually air) is known as free surface problems. This term stems from the fact that the interface is *free* to move with the evolution of the system. The actual form of the free surface boundary is one of the unknowns in these problems, hence determining the shape of the free surface is part of the solution.

In general, free surfaces obey the Bernoulli principle, which yields a nonlinear boundary condition along the free surface. This nonlinear condition, coupled with the unknown form of the free surface, rapidly reduces the tractability of free surface problems, especially in terms

of calculating analytical solutions. In order to overcome this difficulty, numerous methods have been employed to simplify free-surface problems. These methods have often involved various approximations and numerical schemes. Ideally, one wishes to employ a method that treats the free surface problem analytically as far as possible, while only resorting to numerical schemes in the final stages of the solution, which naturally produces more accurate results.

One such method is to employ the feasible assumptions that the flow is irrotational, and the fluid is incompressible and inviscid, which is the approach used in this thesis. These assumptions lead to the system obeying Laplace's equation everywhere within the domain except in the neighbourhood of singularities such as sources and sinks. This allows two-dimensional problems to be treated analytically with complex analysis and boundary integral methods, whilst numerical methods are only employed to solve the resultant integral equations.

## 1.2 Flow due to a submerged source or sink

One particular problem of interest is that of a steady flow system due to a line source or sink in a channel of fluid of finite depth and infinite length. Hocking [1] discusses how these flow models can be used to study the pumping and draining of various bodies of water such as reservoirs, cooling ponds or solar ponds, which usually do not consist of homogeneous fluid but rather a number of stratified layers. The fluid stratification is a direct result from the varying densities of the fluid, which arise from temperature gradients and contaminant concentrations.

Particularly in reservoirs, a layer of fresh water usually overlays a deeper layer, which may contain unwanted salts and pollutants. As a result, it is often imperative that management carefully controls the rate of water withdrawal in such a manner that the neighbouring fluid is not drained [2]. Such controlled procedures may be used, for example, to remove a lower layer of polluted water in a reservoir, and leave the remaining uncontaminated water. In addition, controlled withdrawal and inflow of solar ponds may be used to manage the fluid stratification, which stabilizes and optimizes the system [1].

The solutions of such free surface problems also has a scientific interest as many rudimentary questions in this area remain unanswered. Finally, it should be noted that similar fluid flow models can be used to describe other flow systems such as flow under a boat bow [3]

or a sluice gate [4], and accordingly, similar conformal mapping and numerical methods are applicable for these related problems. We discuss the relationship between the problem of flow due to a source or sink with the related problems further in Section 7.2.

We are interested in the steady state form of the free surface, with particular interest in whether or not wave formation occurs on the free surface when the system is under the effect of gravity. The flow of such systems is characterized by the Froude number, $F$, defined in general as

$$F = \frac{m}{\sqrt{gL^3}},$$

where $m$ is the flux in the far field due to the source, $g$ is the acceleration due to gravity and $L$ is a typical length of the system. The value for the typical length differs depending on which Froude number is desired. The Froude number which uses the average height of the fluid in the far field as the typical length is known as the depth-based Froude number, $F_B$. One important factor of this characteristic number is its ability to predict whether or not wave-formation is possible for this type of problem.

It can be shown (see Stoker [5] or Debnath [6], for example) for flow systems that waves cannot occur on free surfaces when $F_B > 1$ while waves can occur when $F_B < 1$. These types of flow systems are known as *supercritical* and *subcritical*, respectively. It should be noted that while this terminology originates from the linear theory of water waves, their definitions have evolved to described nonlinear wave phenomena.

The problem presented here is that of a subcritical system, which has gained some interest in recent years. One early solution of note was obtained by Hocking and Forbes [7]. This solution laid down the foundation for the analysis to be performed here by using a classic boundary integral method in a conformally mapped plane to solve a system with low Froude numbers. This solution, however, failed to predict waves of any size on the free surface.

During the same year, Mekias and Vanden-Broeck [8] used a slightly different method, which involved reflecting the system along the channel bottom before applying the boundary integral. Their results disagreed with those of Hocking and Forbes [7] by showing that a train of waves did actually occur upstream on the free surface. The numerical results suggested that the amplitude of the waves became exponentially small as $F_B$ approached zero.

Vanden-Broeck [9] attempted to reconcile the conflicting results by employing Hocking and Forbes' solution method to solve the problem. The results agreed with that of Mekias

and Vanden-Broeck [8] by showing a train of waves exists on the free surface. Additionally, it was shown that for lower Froude numbers, the waves were so small that the free surface was effectively flat, agreeing with the profiles of Hocking and Forbes [7].

Finally, Hocking and Forbes [10] employed another boundary integral method similar to that of Hocking and Forbes [7] but with surface tension taken under consideration. While, surface tension shall be neglected here, the results also showed that waves were possible on the free surface. This type of solution is of interest as it offers a viable solution method in solving the problem presented here.

The well-established methods [11] used here will follow the lead of Hocking and Forbes solutions [7, 10] and Vanden-Broeck [9]. The solution methods all involved conformal mapping and boundary integral methods in order to produce a more tractable problem. The final nonlinear equations obtained will need to be solved numerically with a nonlinear minimization methods such as Newton-Raphson or Levenberg-Marquardt scheme.

## 1.3 Goals of this project

This project is concerned with the free surface flow that arises if a line source is placed beneath the surface of a fluid in a channel of finite-depth. This problem has been considered previously in the literature by Hocking and Forbes [7], Mekias and Vanden-Broeck [8], Vanden-Broeck [9] and Hocking and Forbes [10]. In particular, we wish to achieve the following goals:

- We shall work through the formulation of the problem, giving a clear account of the assumptions made, and their consequences. This work shall be presented in Chapter 2.

- The problem will be reformulated in Chapter 3 using a series of conformal maps following the work of [7], [9] and [10]. The entire nonlinear free boundary problem will be reduced to solving a nonlinear singular integral equation.

- A number of small but significant errors exist in the paper by Hocking and Forbes [10]. One of our goals is to rectify these errors and clarify any misconceptions that may exist, and to present a correct, readable and lucid account of the problem formulation and solution.

- We shall solve the singular integral equation using a numerical scheme analogous to [7], [9] and [10]. This is already a significant challenge given the nonlinear nature of the problem, however much of the detail is left out of these papers, and as such there are a number of issues that need clarifying and amending. This part of the project will be detailed in Chapter 4.

- Once the code is working the goal is to run the program a number of times using various Froude numbers in order to vindicate the results of the Vanden-Broeck [8, 9] by showing the numerical existence of a wave-train upstream on the free surface. Furthermore, we wish use the numerical scheme to derive a relationship between wave amplitude and the upstream Froude number, and confirm that the amplitude of the waves is exponentially small in the limit of small Froude number. These results will be presented in Chapter 6, with the code given in Appendix A.

- It is possible to use a regular perturbation scheme to derive an asymptotic solution in the limit that the Froude numbers approaches zero. This approach was used by Hocking and Forbes [7], who calculate the leading order term only. One of the goals of the project is to confirm the leading order solution of [7], and to extend this result by calculating the correction term. We include this calculation in Chapter 5.

- The question of whether or not waves occur on the free surface is very important for a number of reasons, as will discussed in Chapter 7. A long term goal for researchers in this area is to use asymptotic analysis to prove that waves always exist on the free surface for the class of problems considered in this project, no matter how small the Froude number is. Such an analysis must be capable of capturing exponentially small terms, unlike the perturbation scheme given by Hocking and Forbes [7] (and extended in Chapter 5). It is likely that these terms will be *beyond all orders*, and thus will require *exponential asymptotics*, a highly sophisticated theory which has made enormous advances in recent years (see Boyd [12]). We shall discuss this possibility and outline the how exponential asymptotics could be used in the present problem in Chapters 5 and 7.

- Finally, a goal is to put the problem of free surface flow due to a line source into a greater context by relating it to other problems in hydrodynamics such as flow past the bow or stern of a ship and flow past a sluice gate in Chapter 7.

# Chapter 2

# Mathematical Formulation

In this chapter we shall outline our physical assumptions, which have been made to simplify the problem of a flow system and to present a more tractable mathematical model. The governing equations and boundary conditions of the model shall be developed. Finally, we shall nondimensionalize all variables, a process that will reveal the number of independent parameters in the problem.

## 2.1 Physical assumptions

Our flow system consists of a layer of water with a layer of air above it. It is assumed that the viscosity of the water can be neglected thus the water is considered to be *inviscid*. This is effectively equivalent to saying the viscous forces are much smaller than the inertial forces, or that the *Reynolds number* is large, which is certainly the case for withdrawal problems. We assume that density of the water is constant and thus the fluid is *incompressible*. Although in reality water is compressible to a certain extent, its density variation on the scale used in withdrawal problems is negligible. Finally, we suppose that the flow system has started from rest at some initial time, so that initially the vorticity of the fluid was zero. Since the vorticity in an inviscid, incompressible fluid in constant along a streamline, if it is initially zero then it is always so. Hence the flow is considered to be *irrotational*. All of these assumptions are standard, and are explained in further detail in classic texts such as Batchelor [13] and Milne-Thomson [11].

## 2.2 Problem description

The steady system consists of the irrotational flow of an inviscid, incompressible fluid in a finite-depth channel, under the effect of gravity, $g$. The symmetrical flow-domain is bounded above by a free surface and below by a horizontal bottom. A line source of strength $2m$ (that is $m$ is the flux in the far field) is located beneath the surface. It is assumed that directly above the submerged source on the free surface a stagnation point exists where the fluid velocity is zero. This assumption is based on the perfect symmetry of the system.

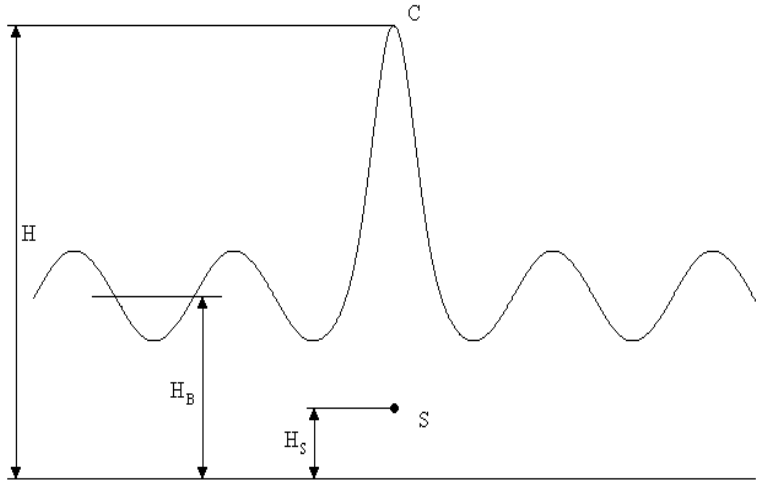


Figure 2.1: 2-D profile of stagnation point with submerged source.

Due to a quadratic source term that arises later in the dynamic boundary condition, the solution methods outlined here should apply equally to problems involving sources or sinks. However, there is an important exception. If the flow is due to a sink, then it is not physically possible for a train of waves to exist on the free surface in the far field. This intuitive requirement, known as the *Sommerfield radiation condition*, can be derived mathematically by showing that the group velocity for water waves is always smaller than the phase velocity (see Stoker [5] or Debnath [6], say). Henceforth, we shall refer to the singularity as a source while taking note that the treatment applies similarly to sinks as well when the Sommerfield radiation condition is satisfied.

In a similar manner to Vanden-Broeck [9], the physical plane has its origin located at the stagnation point $C$, and is located at a height of $H$ from the channel bottom. The average height of the free surface upstream and the height of the source are denoted by $H_B$ and $H_S$

respectively.

## 2.3 Governing equations

In nondimensional variables, we introduce the fluid velocity vector, $\mathbf{q} = u\mathbf{i} + v\mathbf{j}$, which is related to the vorticity vector, $\boldsymbol{\omega}$, by the curl expression

$$\nabla \times \mathbf{q} = \boldsymbol{\omega}. \tag{2.1}$$

The vorticity of the system is a measurement of the rate of rotation of a fluid particle about the axes (Batchelor [13]). Since we assume that the flow system is irrotational the vorticity vanishes, which reduces equation (2.1) to

$$\nabla \times \mathbf{q} = 0. \tag{2.2}$$

This result implies that the velocity vector can be written as

$$\mathbf{q} = \nabla\phi, \tag{2.3}$$

where $\phi$ is known as the velocity potential of the system [14]. From vector calculus, the velocity potential along path $S$ is expressed as

$$\phi = \int_S \mathbf{q} \cdot \mathbf{dr}. \tag{2.4}$$

We safely assume that the systems obeys the conservation of matter which corresponds to a zero divergence

$$\nabla \cdot \mathbf{q} = 0,$$

which together with equation (2.3) leads to the linear Laplace equation, namely

$$\nabla \cdot (\nabla\phi) = \nabla^2\phi = 0. \tag{2.5}$$

It is well-established that working with the scalar quantities such as $\phi$, instead of vector quantities, markedly simplifies the solution method [11]. Hence, this approach has been employed here.

## 2.4 Kinematic conditions

Naturally, the flow of fluid does not cross the free surface or channel bottom. Since the fluid must flow along the boundaries, the angle of the flow between the horizon, $\delta$, is simply the angle of the fluid velocity $\mathbf{q}$ along these streamlines. This angle is obtained in a straightforward manner by using the relation

$$\tan(\delta) = \frac{\bar{v}}{\bar{u}},$$

where $\bar{u}$ and $\bar{v}$ are the respective horizontal and vertical components of the fluid velocity. Note that the bars denote dimensional variables. The angle of the fluid velocity along the streamlines is just a measurement of the gradient,

$$\tan(\delta) = \frac{d\bar{y}}{d\bar{x}}$$

of any boundary line. Additionally, dimensional Cartesian variables $\bar{x}$ and $\bar{y}$ have been introduced and bars have been employed to signify which variables have dimensions. These relations lead to the following kinematic condition being held along all boundaries,

$$\bar{v} = \bar{u}\frac{d\bar{y}}{d\bar{x}}. \tag{2.6}$$

Along the channel bottom the vertical component of the fluid velocity is zero, which yields the following kinematic condition

$$\bar{v} = 0, \quad \bar{y} = -H. \tag{2.7}$$

## 2.5 Dynamic conditions

For a steady flow of an inviscid fluid under the effect of gravity, the well-established Bernoulli equation [13] describes the system

$$\frac{1}{2}\bar{q}^2 + \frac{p}{\rho} + g\bar{y} = K, \tag{2.8}$$

where $p$ and $\rho$ are the fluid pressure and density respectively, and $K$ is some constant of the system. We have assumed that the air pressure exerted upon the free surface of the water is constant, which is not strictly true in reality but the minute pressure variation on this scale can be neglected. The nonlinear condition (2.8) is held everywhere within the flow domain.

The fluid velocity at the stagnation point is naturally equal to zero, thus if we apply the Bernoulli equation at the stagnation point (that is, on the free surface where $\bar{x} = 0, \bar{y} = 0$), the equation reduces to the following fluid-surface condition

$$\frac{p_A}{\rho} = K,$$

where $p_A$ is the atmospheric pressure experienced anywhere on the free surface. This condition states that the pressure along the entire free surface is constant. By substituting this result into the original equation (2.8), the Bernoulli equation for anywhere along the free surface is expressed as

$$\frac{1}{2}\bar{q}^2 + g\bar{y} = 0. \tag{2.9}$$

## 2.6 Nondimensionalizing

For mathematical treatment, system variables need to be nondimensionalized. Distances and velocities shall be nondimensionalized with respect to $H$ and $m/H$, respectively. The bars on all nondimensionalized variables shall be removed to show that they are indeed dimensionless. In this fashion, the Cartesian coordinates, the fluid velocity components and the fluid velocity, respectively, become

$$x = \frac{\bar{x}}{H}, \quad y = \frac{\bar{y}}{H}, \quad u = \frac{\bar{u}H}{m}, \quad v = \frac{\bar{v}H}{m}, \quad q = \frac{\bar{q}H}{m}.$$

The average upstream depth and the height of the source are denoted by $\gamma$ and $\mu$ respectively. In nondimensional variables, the flux in the far field and the height of the stagnation point are both equal to unity.

The new dimensionless variables are substituted into equation (2.9) to yield

$$\frac{1}{2}\left(\frac{qm}{H}\right)^2 + gHy = 0$$

and the expression is divided through by $H$ and $g$ to obtain the nondimensional Bernoulli equation

$$\frac{1}{2}\left(\frac{m^2}{gH^3}\right)q^2 + y = 0, \tag{2.10}$$

which is to be applied on the free surface.

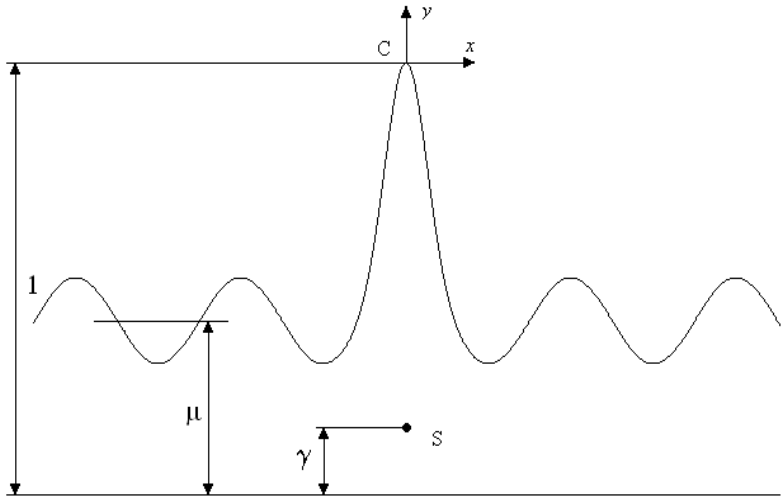


Figure 2.2: Profile of the free surface problem with nondimensional variables.

## 2.7 Froude numbers

The depth-based Froude number was discussed earlier in regards to its ability to predict the possibility of wave-formation. In its complete form it is expressed as

$$F_B = \frac{m}{\sqrt{gH_B^3}}. \tag{2.11}$$

The Froude number that uses the stagnation-point height as its typical length is denoted by $F_{SP}$ and is similarly expressed as

$$F_{SP} = \frac{m}{\sqrt{gH^3}}. \tag{2.12}$$

After some algebraic manipulation and the use of dimensionless variables in equation (2.11), a relation between the two Froude numbers is ascertained to be

$$F_B = \frac{m}{\sqrt{gH_B^3}} = \frac{m}{\sqrt{gH}}\sqrt{\frac{H^3}{H_B^3}} = \frac{F_{SP}}{\mu^{3/2}}. \tag{2.13}$$

Inspection of equation (2.10) reveals that the nondimensional term $\frac{m^2}{gH^3}$ is simply the square of the stagnation-point Froude number, which reduces the Bernoulli equation to

$$\frac{1}{2}F_{SP}^2 q^2 + y = 0, \tag{2.14}$$

a condition satisfied along the free surface.

## 2.8 Summary

We have considered the problem of the flow due to a line source with a stagnation point on the free surface. The problem has been nondimensionalized so that the stagnation point is located at the origin, and the source is at the point $(x, y) = (0, -1 + \gamma)$. The flow is bounded below by a horizonal bottom at $y = -1$, and far downstream the average level of the fluid is located at $y = -1 + \mu$.

The system can be effectively described by the nondimensional quantity $\phi$, which is a velocity potential. From our assumptions that the fluid is incompressible and inviscid and that the flow is irrotational, we established that $\phi$ satisfies Laplace's equation

$$\nabla^2 \phi = \frac{\partial^2 \phi}{\partial x^2} + \frac{\partial^2 \phi}{\partial y^2} = 0, \tag{2.15}$$

throughout the flow domain, except at the source, where it behaves like

$$\phi \sim \frac{1}{2\pi} \log[x^2 + (y + 1 - \gamma)^2] \quad \text{as} \quad (x, y) \to (0, -1 + \gamma). \tag{2.16}$$

On the horizonal bottom we have the boundary condition

$$\frac{\partial \phi}{\partial y} = 0, \quad y = -1, \tag{2.17}$$

while on the free surface we have the two boundary conditions

$$\frac{\partial \phi}{\partial y} = \frac{\partial \phi}{\partial x} \frac{dy}{dx}, \tag{2.18}$$

$$\frac{1}{2} F_{SP}^2 \left| \nabla \phi \right|^2 + y = 0, \tag{2.19}$$

where the parameter $F_{SP}$ is the Froude number. Note that the problem is nonlinear because of the unknown free surface as well as the nonlinear nature of the last boundary condition, Bernoulli's equation. There is, not surprisingly, no analytical solution to this problem; however we can solve it using a combination of analytic and numerical techniques, and these are described in the following chapters.

# Chapter 3

# Boundary Integral Method

In the previous chapter we derived the governing equations for our problem, including Laplace's equation and appropriate boundary conditions pertaining to our physical assumptions of the flow system. In the present chapter we shall formulate the problem with the use of complex variable theory to describe our model, and simplify the geometry with the use of conformal mapping. A boundary integral method is then used to derive an integral equation, which describes our problem completely.

## 3.1 Complex variables

We have established that the flow of the system presented here obeys the equation $\mathbf{q} = \nabla\phi$, within the flow domain except at the source, which implies

$$u = \frac{\partial\phi}{\partial x}, \quad v = \frac{\partial\phi}{\partial y}. \tag{3.1}$$

We introduce the quantity $\psi$, known as the stream function, defined by

$$u = \frac{\partial\psi}{\partial y}, \quad v = -\frac{\partial\psi}{\partial x}. \tag{3.2}$$

We combine equations (3.1) and (3.2) to yield the well-renowned Cauchy-Riemann equations [15], namely

$$\frac{\partial\phi}{\partial x} = \frac{\partial\psi}{\partial y}, \quad \frac{\partial\phi}{\partial y} = -\frac{\partial\psi}{\partial x}. \tag{3.3}$$

We can introduce complex analysis and use a complex potential function to describe the system [11]. We let the complex variable $z = x+iy$ represent the physical plane and introduce

the complex potential

$$f(z) = \phi(x, y) + i\psi(x, y), \tag{3.4}$$

which, since $\phi$ and $\psi$ obey the Cauchy-Riemann equations, is an analytic function of $z = x+iy$ everywhere within the flow domain except at the source.

The line source is a mathematical singularity [15], and as a result, the complex potential $f(z)$ is not analytic there. In the neighbourhood of the source the potential is given by

$$f(z) \sim \frac{1}{\pi} \ln(z - z_0) \quad \text{as} \quad z \to z_0,$$

where $z_0$ marks the position of the source on the complex plane. Using the nondimensional variables, the above expression becomes

$$f(z) \sim \frac{1}{\pi} \ln(z + 1 - \gamma) \quad \text{as} \quad z \to \gamma - 1. \tag{3.5}$$

We introduce the complex conjugate velocity, $w$ expressed as

$$f'(z) = w(z) = u - iv, \tag{3.6}$$

which also is an analytic function. The complex velocity is related to the fluid velocity simply by

$$w = qe^{-i\delta}. \tag{3.7}$$

where $\delta$ is the aforementioned angle of the velocity vector in relation to the horizontal axis and $q = \sqrt{u^2 + v^2}$ is the magnitude of the velocity.

## 3.2 Symmetry of the system

It is been assumed that the problem presented here is perfectly symmetric about the $y$-axis. This symmetry allows the problem to be simplified by only treating one side of the system. The right-hand side half is arbitrarily chosen for analysis, which corresponds to the source strength becoming $m$.

The reflection process here is physically akin to inserting a vertical wall of infinitesimal width directly in the centre of the system thus creating two mirrored systems. Hence, we shall now assume that a solid boundary exists to the left side. Naturally, when solutions are obtained for the right-hand side, it is a straightforward process of reflecting the results in order to gain a physical description of the whole system.

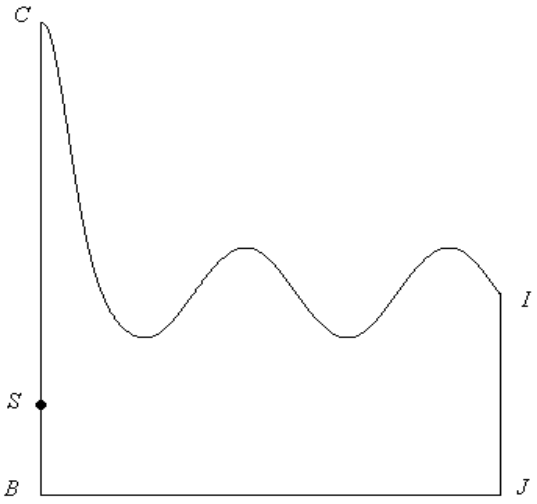


Figure 3.1: Right-hand side of problem with a solid boundary located to the left.

## 3.3 Potential function

All known values of the potential function for the system need to be plotted onto the $f$-plane. While maintaining the system's generality, we let $\psi = 0$ on the free surface and $\phi = 0$ at the stagnation point, $C$.

With the $f$ values set for the stagnation point, we now investigate the potential values along the channel bottom, in particular directly beneath the source at point $B$. By integrating equation (3.2) up to the $x$-axis, we obtain a general expression for the stream function

$$\psi = -\int_y^0 u dy' + k(x) + c,$$

where $y'$ is a dummy variable, $c$ and $k(x)$ is a constant and function of $x$ due to integration. Since the stream function is constant anywhere along the channel bottom, regardless of the $x$ value, the function $k(x)$ disappears. Intuitively, since the stream function was set to zero at the origin, the integration constant must be zero, which reduces the equation to

$$\psi = -\int_y^0 u dy'.$$

Upon inspection, we observe that the integral is simply the negative of the flux across the defined region. From the conservation of mass, we know that the total flux must be equal to the dimensionless source strength, which is equal to one. Thus, $\psi = -1$ anywhere along the channel bottom.

At point $B$, the value of $\phi$ is unknown and is denoted as $\phi_B$, and is arbitrarily placed on the left-hand side of the $f$-plane.

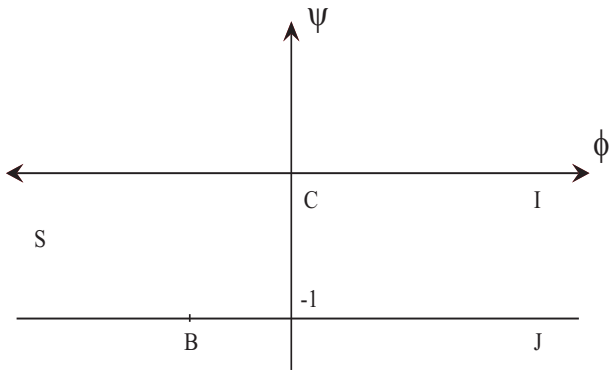


Figure 3.2: The problem on the $f$-plane.

The location of the source at point $C$ on the $f$-plane is obtained with a physical argument. It is known that the source is a singularity, and thus, the the velocity of fluid leaving the source has effectively an infinite speed, which corresponds to point $S$ being located at negative infinity on the $\phi$-axis. Finally, all fluid in the system originates from the source, hence all streamlines do as well. All streamlines spread out between the free surface and the channel bottom. Since the stream function values are known for the boundaries, intuitively the values for $\psi$ at the source must range from 0 to $-1$.

## 3.4 Mapping the potential

All the points of the system are now located on the infinite strip between $\psi = 0$ and $\psi = -1$ on the $f$-plane. In order to reformulate this problem using a boundary integral method we introduce the complex variable $\zeta = \xi + i\eta$, allowing the infinite strip to be mapped onto the lower-half of the $\zeta$-plane with the conformal transformation

$$\zeta = \xi + i\eta = e^{\pi f}. \tag{3.8}$$

Point C is located at $\phi = 0$ and $\psi = 0$ on the $f$-plane, which corresponds to

$$\zeta = \xi_C = 1.$$

Point B is located at $\phi = \phi_B$ and $\psi = -1$ on the $f$-plane, which corresponds to

$$\zeta = \xi_B = -e^{\pi\phi_B}.$$

Point I is located at $\phi = \infty$ and $\psi = 0$ on the $f$-plane, which corresponds to

$$\zeta = \xi_I = \infty + 0i.$$

Point J is located at $\phi = \infty$ and $\psi = -1$ on the $f$-plane, which corresponds to

$$\zeta = \xi_J = -\infty + 0i.$$

Point S is located at $\phi = -\infty$ and between $\psi = 0$ and $\psi = -1$ on the $f$-plane, which corresponds to

$$\zeta = \xi_S = 0.$$

All points of importance are located on the real axis on the $\zeta$-plane. The free surface corresponds to $1 < \xi < \infty$ while the channel bottom corresponds to $-\infty < \xi < \xi_B$. The wall is divided into two sections: beneath the source corresponds to $\xi_B < \xi < 0$ while above the source corresponds to $0 < \xi < 1$.

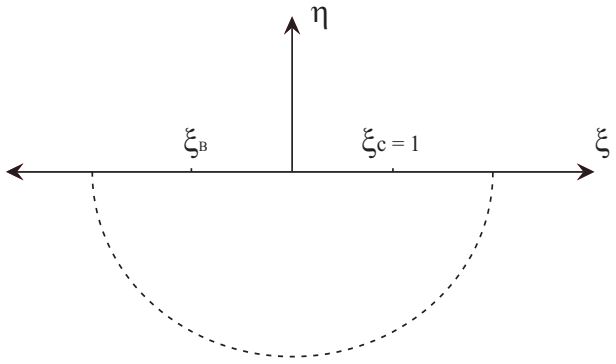


Figure 3.3: The problem mapped to the lower half of the $\zeta$-plane.

## 3.5 Logarithmic hodograph

The governing equations need to be reformulated for the $\zeta$-plane with the geometry of the system embedded. We introduce a new analytic function, known as the logarithmic hodograph [3], defined as

$$\Omega(\zeta) = \delta(\zeta) + i\tau(\zeta), \tag{3.9}$$

which is related to the complex velocity (3.6) by

$$f'(z(\zeta)) = u - iv = \frac{1}{\mu} e^{-i\Omega(\zeta)} \tag{3.10}$$

where $\mu$ is the nondimensional average depth of the fluid upstream. In order to gain some physical interpretation of the function, we recast it in the following form

$$w = u - iv = \frac{1}{\mu} e^{\tau(\zeta)} e^{-i\delta(\zeta)}. \tag{3.11}$$

By comparing result (3.11) to equation (3.7), we observe that $q = \frac{1}{\mu} e^{\tau(\zeta)}$ and $\delta = \delta(\zeta)$. Thus, $\frac{1}{\mu} e^{\tau(\zeta)}$ gives the magnitude of the fluid velocity and $\delta(\zeta)$ gives the angle between the streamlines and the $x$-axis.

## 3.6 Boundary values

As previously discussed, the kinematic conditions ensure that the fluid flow follows the boundaries of the system. Hence, the physical interpretation of $\delta(\zeta)$ along the boundaries is the actual angle of the the solid boundaries to the horizonal. Further, along the boundaries the complex variable $\zeta$ takes real values $\xi$. Thus, by inspecting the orientation of the different boundaries on the physical plane, the values of $\delta(\xi)$ are obtained for all the $\xi$ values that correspond to solid boundaries, as follows:

$$\delta(\xi) = \begin{cases} 0 & \text{if} \quad -\infty < \xi < \xi_B, \\ -\pi/2 & \text{if} \quad \xi_B < \xi < 0, \\ \pi/2 & \text{if} \quad 0 < \xi < 1, \\ \text{unknown} & \text{if} \quad 1 < \xi < \infty. \end{cases} \tag{3.12}$$

## 3.7 Cauchy's Theorem

An equation that relates $\tau(\xi)$ and $\delta(\xi)$ on the real axis can be ascertained by applying a circular integral of the function $\Omega(\zeta)$ around the curve denoted by $\Gamma$ in an anti-clockwise direction. With the singularity on the exterior of the integral region, we invoke the famous Cauchy integral theorem [16], namely

$$\oint_\Gamma \frac{\Omega(\zeta)}{\zeta - \zeta_0} d\zeta = 0, \tag{3.13}$$

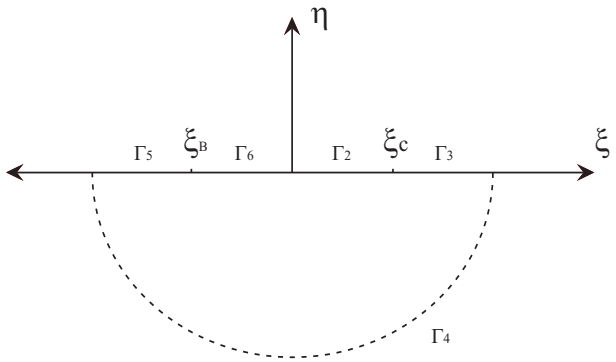


Figure 3.4: The semi-circle $\Gamma$ separated into different regions on the $\zeta$-plane.

where $\zeta_0$ is a point outside $\Gamma$. In fact we let $\zeta_0$ lie on the real axis. The singular point $\zeta_0 = \xi_0$ is avoided by forming a detour in the shape of a semi-circle of vanishing radius around it denoted by $\Gamma_1$. We use the residue theorem [14] to obtain the integral contribution of the $\Gamma_1$, namely

$$\int_{\Gamma_1} \frac{\Omega(\zeta)}{\zeta - \xi_0} d\zeta = i\pi\Omega(\xi_0).$$

Also, the integral contribution of the semi-circle of infinite radius, denoted by $\Gamma_4$, yields

$$\int_{\Gamma_4} \frac{\Omega(\zeta)}{\zeta - \xi_0} d\zeta = 0.$$

These results are substituted into equation (3.13) to give

$$\Omega(\xi_0) = \frac{i}{\pi} \barint_{-\infty}^{\infty} \frac{\Omega(\xi)}{\xi - \xi_0} d\xi, \tag{3.14}$$

which by taking the real and imaginary parts give

$$\tau(\xi_0) = \frac{1}{\pi} \barint_{-\infty}^{\infty} \frac{\delta(\zeta)}{\xi - \xi_0} d\xi, \tag{3.15}$$

$$\delta(\xi_0) = -\frac{1}{\pi} \barint_{-\infty}^{\infty} \frac{\tau(\xi)}{\xi - \xi_0} d\xi, \tag{3.16}$$

where the bars denote Cauchy Principal Values. The integral region in equation (3.15) is broken into separate integral regions marked as follows:

| Region | $\xi$ Lower Limit | $\xi$ Upper Limit |
|---|---|---|
| II | 0 | 1 |
| III | 1 | $\infty$ |
| V | $-\infty$ | $\xi_B$ |
| VI | $\xi_B$ | 0 |

Thus, the integral in equation (3.15) is broken into four integrals

$$\begin{aligned}\tau(\xi_0) &= \int_{\Gamma_2} \frac{\delta(\xi)}{\xi-\xi_0}d\xi + \int_{\Gamma_3} \frac{\delta(\xi)}{\xi-\xi_0}d\xi + \int_{\Gamma_5} \frac{\delta(\xi)}{\xi-\xi_0}d\xi + \int_{\Gamma_6} \frac{\delta(\xi)}{\xi-\xi_0}d\xi \\ &= \frac{1}{\pi}\int_0^1 \frac{\delta(\xi)}{\xi-\xi_0}d\xi + \frac{1}{\pi}\int_1^\infty \frac{\delta(\xi)}{\xi-\xi_0}d\xi + \frac{1}{\pi}\int_{-\infty}^{\xi_B} \frac{\delta(\xi)}{\xi-\xi_0}d\xi + \frac{1}{\pi}\int_{\xi_B}^0 \frac{\delta(\xi)}{\xi-\xi_0}d\xi.\end{aligned}$$

The $\delta(\xi)$ values are known for regions II, V, and VI from the flow conditions (3.12). Substitution of these values gives

$$\tau(\xi_0) = \frac{1}{\pi}\int_0^1 \frac{\pi/2}{\xi-\xi_0}d\xi + \frac{1}{\pi}\int_1^\infty \frac{\delta(\xi)}{\xi-\xi_0}d\xi + \frac{1}{\pi}\int_{\xi_B}^0 \frac{-\pi/2}{\xi-\xi_0}d\xi, \tag{3.17}$$

leaving the remaining two integrals to be evaluated. The integral for region II yields

$$\frac{1}{\pi}\int_0^1 \frac{\pi}{2}\frac{1}{\xi-\xi_0}d\xi = \frac{1}{2}\ln\left(\frac{1-\xi_0}{-\xi_0}\right), \tag{3.18}$$

while the integral for region VI yields

$$\frac{1}{\pi}\int_{\xi_B}^0 \frac{-\pi}{2}\frac{1}{\xi-\xi_0}d\xi = \frac{1}{2}\ln\left(\frac{\xi_B-\xi_0}{-\xi_0}\right). \tag{3.19}$$

Addition of results (3.19) and (3.18) gives

$$\frac{1}{\pi}\int_0^1 \frac{\delta(\xi)}{\xi-\xi_0}d\xi + \frac{1}{\pi}\int_{\xi_B}^0 \frac{\delta(\xi)}{\xi-\xi_0}d\xi = \frac{1}{2}\ln\left[\frac{(1-\xi_0)(\xi_B-\xi_0)}{\xi_0^2}\right]$$

This result is substituted into the original integral (3.17) to obtain the expression

$$\tau(\xi_0) = \frac{1}{2}\ln\left[\frac{(\xi_0-1)(\xi_0-\xi_B)}{\xi_0^2}\right] + \frac{1}{\pi}\int_1^\infty \frac{\delta(\xi)}{\xi-\xi_0}d\xi.$$

The variables are aptly changed to obtain the equation

$$\tau(\xi) = \frac{1}{2}\ln\left[\frac{(\xi-1)(\xi-\xi_B)}{\xi^2}\right] + \frac{1}{\pi}\int_1^\infty \frac{\delta(\xi')}{\xi'-\xi}d\xi', \qquad \xi > 1. \tag{3.20}$$

This equation effectively describes the magnitude of the fluid velocity for a point located anywhere along the free surface corresponding to $1 < \xi < \infty$ on the $\xi$-axis.

Equation (3.20) is valid for $\xi > 1$ and as such gives real values in this $\xi$ range. To calculate $\tau(\xi)$ values for $\xi_B < \xi < 1$ we need to modify equation (3.20) slightly. When $\xi_B < \xi < 1$ equation (3.20) gives complex values due to its log term, or more specifically the square root in the log term. To rectify this we factor out and completely remove a negative one from the the log term

$$\frac{1}{2}\ln\left[\frac{(\xi-1)(\xi-\xi_B)}{\xi^2}\right] = i\pi + \frac{1}{2}\ln\left[\frac{(1-\xi)(\xi-\xi_B)}{\xi^2}\right]$$

Recall that one of the steps in deriving equation (3.15) involved taking the imaginary part of the equation. Inspection of the equation (3.20) derivation reveals that imaginary the term $i\pi$ in the above expression becomes real during the derivation. This implies that when the imaginary part is taken to yield an equation (3.20), the $\pi$ term is not in equation (3.20). Thus, we can write equation (3.20) as

$$\tau(\xi) = \frac{1}{2}\ln\left[\frac{(1-\xi)(\xi-\xi_B)}{\xi^2}\right] + \frac{1}{\pi}\int_1^\infty \frac{\delta(\xi')}{\xi'-\xi}d\xi', \qquad \xi_B < \xi < 1, \tag{3.21}$$

which is valid since it produces real values. Finally, the singularity of the integral term has been removed due to the change of $\xi$ value range, hence the Cauchy principal integral becomes a regular integral.

## 3.8 Mapping back to the physical plane

Expressions for obtaining the $z$-plane points that lie on the free surface are needed. In order to obtain these expressions, we ascertain an expression for $z$ by rearranging equation (3.10) to give

$$dz = \mu e^{i\Omega(\zeta)}df. \tag{3.22}$$

By differentiating and rearranging the transformation (3.8) we obtain the differential equation

$$\frac{d\zeta}{df} = \pi e^{\pi f} = \pi\zeta,$$

and hence equation (3.22) becomes

$$dz = \mu e^{i\Omega(\zeta)}df = dz = \frac{\mu}{\pi}\frac{e^{i\Omega(\zeta)}}{\zeta}d\zeta.$$

On the boundaries in the physical plane, $\zeta$ is real so the equation reduces to

$$dz = \frac{\mu}{\pi}\frac{e^{i\Omega(\xi)}}{\xi}d\xi.$$

This equation is integrated to yield an expression for $z$, namely

$$z(\xi) = \frac{\mu}{\pi}\int_1^\xi \frac{e^{i\Omega(\xi')}}{\xi'}d\xi' = \frac{\mu}{\pi}\int_1^\xi \frac{e^{-\tau(\xi')+i\delta(\xi')}}{\xi'}d\xi'. \tag{3.23}$$

The identity $e^{i\delta} = \cos\delta + i\sin\delta$ and equation (3.9) are used to obtain respective expressions for $x$ and $y$. By taking the real component of equation (3.23) we obtain the $x$ expression

$$x(\xi) = \frac{\mu}{\pi}\int_1^\xi \frac{e^{-\tau(\xi')}\cos\delta(\xi')}{\xi'}d\xi'. \tag{3.24}$$

In a similar fashion an expression for $y$ is obtained by taking the imaginary component of equation (3.23) to obtain

$$y(\xi) = \frac{\mu}{\pi} \int_1^{\xi} \frac{e^{-\tau(\xi')} \sin \delta(\xi')}{\xi'} d\xi'. \tag{3.25}$$

## 3.9 Bernoulli's Equation on the $\zeta$-plane

Inspection of the dimensionless Bernoulli equation (2.14) reveals that we need an expression for the quantity $q^2$. From equation (3.11), we know that magnitude of the complex velocity is equal to the magnitude of the fluid velocity, namely

$$q = \frac{1}{\mu} e^{\tau(\xi)},$$

which is simply squared to yield the expression

$$q^2 = \frac{e^{2\tau(\xi)}}{\mu^2}. \tag{3.26}$$

Equations (3.26) and (3.25) are substituted into equation (2.14) to yield the Bernoulli equation for the $\zeta$-plane, namely

$$\frac{1}{2} F_{SP}^2 \frac{e^{2\tau(\xi)}}{\mu^2} + \frac{\mu}{\pi} \int_1^{\xi} \frac{e^{-\tau(\xi')} \sin \delta(\xi')}{\xi'} d\xi' = 0, \tag{3.27}$$

which applies for $\xi > 1$, corresponding to the free surface.

## 3.10 Nonlinear integral equation

A second equation for $\tau(\xi)$, in addition to (3.20), is derived by differentiating equation (3.27) with respect to $\xi$ and rearranging the results to give

$$\frac{F_{SP}^2}{\mu^2} \frac{d\tau(\xi)}{d\xi} e^{2\tau(\xi)} + \frac{\mu}{\pi} \frac{e^{-\tau(\xi)} \sin \delta(\xi)}{\xi} = 0,$$

which simplifies to

$$\frac{d\tau(\xi)}{d\xi} e^{3\tau(\xi)} + \frac{\mu^3}{\pi F_{SP}^2} \frac{\sin \delta(\xi)}{\xi} = 0.$$

Some algebraic rearrangement and suitable integration is applied to yield

$$\int_1^{\xi} e^{3\tau(\xi')} d\tau(\xi') = -\frac{\mu^3}{\pi F_{SP}^2} \int_1^{\xi} \frac{\sin \delta(\xi')}{\xi'} d\xi'.$$

But the left-hand side of this equation is simply $\frac{1}{3}e^{3\tau(\xi)}$, given that the fluid velocity approaches zero near the stagnation point, implying that $e^{3\tau(\xi)} \to 0$ as $\xi \to 1$. Thus

$$e^{3\tau(\xi)} = -\frac{3\mu^3}{\pi F_{SP}^2} \int_1^\xi \frac{\sin\delta(\xi')}{\xi'} d\xi',$$

or

$$\tau(\xi) = \frac{1}{3} \ln \left[ -\frac{3\mu^3}{\pi F_{SP}^2} \int_1^\xi \frac{\sin\delta(\xi')}{\xi'} d\xi' \right]. \tag{3.28}$$

Equations (3.20) and (3.28) are equated to yield a singular nonlinear integral equation

$$\frac{1}{2} \ln \left[ \frac{(\xi-1)(\xi-\xi_B)}{\xi^2} \right] + \frac{1}{\pi} \fint_1^\infty \frac{\delta(\xi')}{\xi'-\xi} d\xi' = \frac{1}{3} \ln \left[ -\frac{3\mu^3}{\pi F_{SP}^2} \int_1^\xi \frac{\sin\delta(\xi')}{\xi'} d\xi' \right], \tag{3.29}$$

which is valid for $\xi > 1$, that is, anywhere along the free surface.

The integral equation (3.29) is a type of Nekrasov equation, as discussed in Tuck [3] and Wehausen and Laitone [17]. A solution to (3.29) for $\delta(\xi)$ will automatically satisfy Laplace's equation (2.15), since Cauchy's theorem (3.13) works only if $f = \phi + i\psi$ is analytic. The solution will satisfy the singular behaviour (2.16) near the source, as this has been taken care via the conformal mapping. The bottom condition (2.17) and the symmetry of the system is satisfied from substituting the correct value for $\delta$ for $\xi < 1$, as done in equations (3.18) and (3.19). The kinematic condition (2.6) is identically satisfied by forcing $\psi = 0$ on the free surface, as discussed in Section 3.3. Finally, Bernoulli's equation (2.19) is satisfied by any solution to (3.29), as described earlier in this section.

# Chapter 4

# Numerical Scheme

In the previous chapter we derived a singular nonlinear integral equation which governs our problem of flow due to a submerged source. After deriving two additional equations, we shall develop a suitable method to represent and solve these equations for $\delta(\xi)$ and $\mu$, which are then used to determine $\tau(\xi)$. We shall discuss how the singular nature of the integral equations is handled and the briefly outline the details of the numerical scheme. Once the values of $\delta(\xi)$, $\mu$ and $\tau(\xi)$ have been determined, it is a relatively straightforward procedure of calculating the free surface profile with equations (3.24) - (3.25).

## 4.1 System equations

In order to solve the unknown $\delta(\xi)$, $\tau(\xi)$ and $\mu$ values with a suitable numerical scheme, the $\xi$-axis is divided appropriately to yield $N$ mesh points. Since we want these mesh points equally spaced in the physical plane for sufficiently large $x$, we use evenly spaced mesh points in the potential function, $\phi$. Hence, we introduce the change of variables

$$\xi = e^{\pi\phi}. \tag{4.1}$$

The change of variables implies we can rewrite equations (3.20) and (3.28) respectively as

$$\tau(\phi) = \frac{1}{2}\ln\left[\frac{(e^{\pi\phi}-1)(e^{\pi\phi}-e^{\pi\phi_B})}{e^{2\pi\phi}}\right] + \int_0^\infty \frac{\delta(\phi')}{e^{\pi\phi'}-e^{\pi\phi}} e^{\pi\phi'} d\phi', \tag{4.2}$$

$$\tau(\phi) = \frac{1}{3}\ln\left[-\frac{3\mu^3}{F_{SP}^2}\int_0^\phi \sin(\delta(\phi'))d\phi'\right] = 0, \tag{4.3}$$

which naturally transforms equation (3.29) into

$$\frac{1}{2}\ln\left[\frac{(e^{\pi\phi}-1)(e^{\pi\phi}-e^{\pi\phi_B})}{e^{2\pi\phi}}\right]+\fint_0^\infty \frac{\delta(\phi')e^{\pi\phi}}{e^{\pi\phi'}-e^{\pi\phi'}}d\phi'-\frac{1}{3}\ln\left[-\frac{3\mu^3}{F_{SP}^2}\int_0^\phi \sin(\delta(\phi'))d\phi'\right]=0. \quad (4.4)$$

We introduce the evenly spaced mesh points in $\phi$

$$\phi_I=(I-1)\Delta\phi, \quad I=1,...,N, \quad (4.5)$$

where $\Delta\phi$ is a constant spacing of $\phi$ and $N$ is the number of points respectively. The corresponding unknowns are written as

$$\delta_I=\delta(\phi_I), \quad I=1,...,N, \quad (4.6)$$

$$\tau_I=\tau(\phi_I), \quad I=1,...,N. \quad (4.7)$$

It is assumed that the free surface is horizontally flat at the stagnation point, hence $\delta_1=0$. The height of the source above the bottom at point $B$ is an input, and is governed by the value of $\xi_B$ (note that $\xi_B=0$ corresponds to a source on the channel bottom). Thus, there are $N$ unknowns, which are the $\mu$ and $(N-1)$ values of $\delta_I$, to solve.

The integral equation (4.4) is applied at all points between the second and the penultimate point inclusively along the $\xi$-axis. The integral is evaluated with a simple trapezoidal method, which yields $N-2$ nonlinear equations.

A further equation is obtained by slightly modifying equation (3.25), substituting the nondimensional stagnation point height and integrating from $\xi=\xi_B$ to $\xi=\xi_C=1$, which corresponds to the bottom and top of the wall in the physical plane, in order to produce the equation

$$1+\frac{\mu}{\pi}\int_{\xi_B}^1 \frac{e^{-\tau(\xi')}\sin\delta(\xi')}{\xi'}d\xi'=0, \quad (4.8)$$

where the known flow conditions along the wall give $\delta(\xi)$ values for this $\xi$ range. Care must taken due to the singular nature of the integrals and this is discussed in the next section.

The final equation is obtained by using a standard polynomial extrapolation method [18] to relate the last three delta values, namely

$$\delta_N=3\delta_{N-1}-3\delta_{N-2}+\delta_{N-3}. \quad (4.9)$$

Finally, the $\xi_B$ value is a system input and has a value of zero when the source is located on the channel floor. We now have a closed system with $N$ equations and $N$ unknowns to solve.

## 4.2 Singularities

Our derived system of mostly integral equations has a number of singularities that must be treated with care when applying the trapezoidal scheme. It will be shown, by the use of appropriate change of variables, that even though some integrands contain singularities, the integrals are in fact finite in value.

Firstly we must deal the the Cauchy Principle Value integral in (4.4). Following Hocking and Vanden-Broeck [19], we do this by adding and subtracting the singularity as

$$⨍_0^\infty \frac{\delta(\phi')e^{\pi\phi'}}{e^{\pi\phi'}-e^{\pi\phi}}d\phi' = \int_0^\infty \frac{\delta(\phi')-\delta(\phi)}{e^{\pi\phi'}-e^{\pi\phi}}e^{\pi\phi'}d\phi' + \int_0^\infty \frac{\delta(\phi)e^{\pi\phi'}}{e^{\pi\phi'}-e^{\pi\phi}}d\phi'.$$

The first integral on the right-hand side is no longer singular, as the integrand approaches

$$\frac{1}{\pi}\frac{d\delta}{d\phi} \quad \text{as} \quad \phi' \to \phi.$$

as $\phi' \to \phi$. To see this, note that

$$\frac{d\delta}{d\phi} = \frac{d\xi}{d\phi}\frac{d\delta}{d\xi} = \frac{d\xi}{d\phi}\left[\lim_{\xi'\to\xi}\frac{\delta(\xi')-\delta(\xi)}{\xi'-\xi}\right] = \pi e^{\pi\phi}\left[\lim_{\phi'\to\phi}\frac{\delta(\phi')-\delta(\phi)}{e^{\pi\phi'}-e^{\pi\phi}}\right].$$

By using $\phi_N$ as the numerical approximation for infinity (that is, the greatest value $\phi_I$ in the numerical mesh), the integral on the right-hand can be integrated directly to give

$$\int_0^\infty \frac{\delta(\phi)e^{\pi\phi'}}{e^{\pi\phi'}-e^{\pi\phi}}\,d\phi' \approx \delta(\phi)\int_0^{\phi_N}\frac{e^{\pi\phi'}}{e^{\pi\phi'}-e^{\pi\phi}}\,d\phi' = \frac{\delta(\phi)}{\pi}\ln\left[\frac{e^{\pi\phi_N}-e^{\pi\phi}}{e^{\pi\phi}-1}\right],$$

so that we have

$$⨍_0^\infty \frac{\delta(\phi')e^{\pi\phi'}}{e^{\pi\phi'}-e^{\pi\phi}}d\phi' \approx \frac{1}{\pi}\int_0^{\phi_N}\frac{\delta(\phi')-\delta(\phi)}{e^{\pi\phi'}-e^{\pi\phi}}d\xi' + \frac{\delta(\phi)}{\pi}\ln\left[\frac{e^{\pi\phi_N}-e^{\pi\phi}}{e^{\pi\phi}-1}\right]. \tag{4.10}$$

It should be noted that the log of zero does not occur as the above equation is never applied at $\phi_N$.

Now we deal with (4.8), the equation for relating the known height of the physical wall to the other flow variables. By substituting the known values for $\delta$ from (3.12), equation (4.8) becomes

$$1 - \frac{\mu}{\pi}\int_{\xi_B}^0 \frac{e^{-\tau(\xi')}}{\xi'}d\xi' + \frac{\mu}{\pi}\int_0^1 \frac{e^{-\tau(\xi')}}{\xi'}d\xi' = 0.$$

Two singularities arise from the limits of the integral in equation (4.8) corresponding to stagnation points on the physical plane located at the origin and directly below the origin on the channel floor. With the use of (3.21) we have

$$\frac{e^{-\tau(\xi)}}{\xi} = \frac{1}{(1-\xi)^{1/2}(\xi-\xi_B)^{1/2}}\exp\left\{-\frac{1}{\pi}\int_1^\infty \frac{\delta(\xi')}{\xi'-\xi}\,d\xi'\right\} \quad \text{for} \quad \xi_B < \xi < 1,$$

so it's clear that the two stagnation points imply that the integrand blows up at $\xi = \xi_B$ and $\xi = 1$ (but not at $\xi = 0$). To deal with this singular behaviour we make the substitution

$$\xi = \frac{1}{2}[(1 - \xi_B)\sin\theta + 1 + \xi_B],$$

so that

$$\frac{d\xi}{(1-\xi)^{1/2}(\xi - \xi_B)^{1/2}} = d\theta,$$

and hence

$$\begin{aligned}
\frac{e^{-\tau(\xi)}}{\xi}\, d\xi &= \exp\left\{-\frac{1}{\pi}\int_1^\infty \frac{\delta(\xi')}{\xi' - [(1-\xi_B)\sin\theta + 1 + \xi_B]/2}\, d\xi'\right\} d\theta \\
&\approx \exp\left\{-\int_0^{\phi_N} \frac{\delta(\phi')e^{\pi\phi'}}{e^{\pi\phi'} - \frac{1}{2}[(1-\xi_B)\sin\theta + 1 + \xi_B]}\, d\phi'\right\} d\theta \\
&= \exp\{-\Lambda(\theta)\}\, d\theta, \quad \text{say.}
\end{aligned}$$

The change of variable transforms equation (4.8) and its limits of integration accordingly, to the final equation

$$1 - \frac{\mu}{\pi}\int_{-\pi/2}^{\theta_B} e^{-\Lambda(\theta')}d\theta' + \frac{\mu}{\pi}\int_{\theta_B}^{\pi/2} e^{-\Lambda(\theta')}d\theta' = 0, \tag{4.11}$$

where $\theta_B = -\arcsin((1+\xi_B)/(1-\xi_B))$. This new equation has no singularities. However, when numerically calculating $\Lambda(\frac{\pi}{2})$, a division of zero occurs at $\phi_1 = 0$. Fortunately this singularity is removed from the equation as the exponential term in (4.11) reduces the integrand at this point to zero.

## 4.3 Equation solving scheme

We have $N$ unknowns to solve with $N$ nonlinear algebraic equations. In the past the system of equations arising from this type of problem formulation has been usually solved with an iterative Newton-Raphson scheme [7, 9, 10]. Although this method often converges in only a few iterations when it does find the solution, it requires a *good* initial guess or otherwise the scheme will not converge. While the Newton-Raphson scheme is fairly straightforward to implement, each iteration is quite slow to run in *Matlab* since a $N \times N$ matrix of linear equations needs to be solved for each iteration, which is quite computationally exhaustive.

We present alternative solution method by solving the set of $N$ nonlinear equations with the pre-written *Matlab* function *fsolve*, which uses the Gauss-Newton and Levenberg-Marquardt schemes depending on the complexity and nature of the system of equations. As a

rough guide the Gauss-Newton scheme is the default method while the Levenberg-Marquardt scheme is used when the scheme's step length or condition number goes below a certain threshold value [20].

Although these two schemes are both more complex than the Gauss-Newton method, the *fsolve* function is considerably better at solving nonlinear equations. Compared to the Newton-Raphson scheme, the initial guess for *fsolve* can be relatively poor, it takes fewer iterations, and due its pre-written nature and the use of compiled functions, each iteration is done in less time.

As a side note, *fsolve* solves a set of homogeneous equations equations of the form $f_i(x_i) = 0$. The final termination value, determined by the default function tolerance of *fsolve*, varies for each simulation but for our calculations is always less than $10^{-15}$, which offers a very reasonable degree of accuracy for the system.

Thus, we have chosen to solve our system of $N$ nonlinear equations with the *fsolve* function.

## 4.4 Summary

We have $N$ unknowns to solve that consist of the $\delta_I$ values for $I = 2, 3, \ldots, N$, as well as the $\mu$ value. We have derived $N$ nonlinear equations of which $N-2$ are of the form

$$\frac{1}{2}\ln\left[\frac{(e^{\pi\phi}-1)(e^{\pi\phi}-e^{\pi\phi_B})}{e^{2\pi\phi}}\right] + \fint_0^\infty \frac{\delta(\phi')e^{\pi\phi}}{e^{\pi\phi'}-e^{\pi\phi'}}d\phi' - \frac{1}{3}\ln\left[-\frac{3\mu^3}{F_{SP}^2}\int_0^\phi \sin(\delta(\phi'))e^{\pi\phi'}d\phi'\right] = 0,$$

where in order to handle the singularity the integral is expressed as

$$\fint_0^\infty \frac{\delta(\phi')e^{\pi\phi'}}{e^{\pi\phi'}-e^{\pi\phi}}d\phi' \approx \frac{1}{\pi}\int_0^{\phi_N}\frac{\delta(\phi')-\delta(\phi)}{e^{\pi\phi'}-e^{\pi\phi}}d\xi' + \frac{\delta(\phi)}{\pi}\ln\left[\frac{e^{\pi\phi_N}-e^{\pi\phi}}{e^{\pi\phi}-1}\right].$$

A further integral equation, which uses the depth of the channel floor from the stagnation point, was derived as

$$1 - \frac{\mu}{\pi}\int_{-\pi/2}^{\theta_B} e^{-\Lambda(\theta')}d\theta' + \frac{\mu}{\pi}\int_{\theta_B}^{\pi/2} e^{-\Lambda(\theta')}d\theta' = 0,$$

where $\theta_B = -\arcsin((1+\xi_B)/(1-\xi_B))$. The final equation is a simple extrapolation formula relating the last three $\delta$ values to yield

$$\delta_N = 3\delta_{N-1} - 3\delta_{N-2} + \delta_{N-3}.$$

The final derived system of $N$ equations is solved numerically using the equation-solving *Matlab* function, *fsolve*, which utilizes Newton-Gauss and Levenberg-Marquardt schemes [21] and is designed specifically for nonlinear systems [20].

# Chapter 5

# Asymptotic Analysis

In this chapter we shall obtain an exact expression for $\mu$ when there are no waves on the free surface, and apply an asymptotic analysis to the governing integral equation in order to examine the solution of our problem in the limit $F_{SP} \to 0$.

## 5.1 Upstream height for a solution with no waves

The purpose of this section is to calculate the average upstream channel depth when no waves exist upstream on the free surface. In this case the free surface asymptotes to $y = \mu - 1$ as $x \to \infty$ with $q \to \frac{1}{\mu}$ in this limit. These values are substituted into the original nondimensional Bernoulli equation (2.14) to yield

$$\frac{1}{2}\left(\frac{F_{SP}}{\mu}\right)^2 + \mu - 1 = 0,$$

which can be manipulated to obtain the cubic equation

$$\mu^3 - \mu^2 + \frac{1}{2}F_{SP} = 0.$$

This cubic equation is solved using the standard formula (see Abramowitz and Stegun [22]) to yield

$$\mu = \frac{1}{6}\left(8 - 54F_{SP}^2 + 6iF_{SP}\sqrt{24 - 81F_{SP}^2}\right)^{\frac{1}{3}} + \frac{2}{3}\left(8 - 54F_{SP}^2 + 6iF_{SP}\sqrt{24 - 81F_{SP}^2}\right)^{-\frac{1}{3}} + \frac{1}{3},$$

which can be written more compactly in polar form

$$\mu = \frac{1}{6}r^{1/3}e^{i\theta/3} + \frac{2}{3}r^{-1/3}e^{-i\theta/3} + \frac{1}{3}, \tag{5.1}$$

where

$$\theta = \arctan\left(\frac{6F_{SP}\sqrt{24-81F_{SP}^2}}{8-54F_{SP}^2}\right) = \arccos\left(1-\frac{27}{4}F_{SP}^2\right), \tag{5.2}$$

$r^2 = (8-54F_{SP}^2)^2 + 36F_{SP}^2(24-81F_{SP}^2) = 64 - 864F_{SP}^2 + 2916F_{SP}^2 + 864F_{SP}^2 - 2916F_{SP}^2 = 64.$

We use the identity $e^{i\theta} = \cos\theta + i\sin\theta$ to recast equation (5.1) to the form

$$\mu = \left(\frac{1}{6}r^{1/3} + \frac{2}{3}r^{-1/3}\right)\cos\left(\frac{\theta}{3}\right) + i\left(\frac{1}{6}r^{1/3} - \frac{2}{3}r^{-1/3}\right)\sin\left(\frac{\theta}{3}\right).$$

Substituting $r = 8$ simplifies the expression to

$$\mu = \frac{1}{3} + \frac{2}{3}\cos\left(\frac{\theta}{3}\right) = \frac{1}{3} + \frac{2}{3}\cos\left[\frac{1}{3}\arccos\left(1-\frac{27}{4}F_{SP}^2\right)\right]. \tag{5.3}$$

Thus, when there are no waves on the free surface, $\mu$ is given by equation (5.3), otherwise $\mu$ is an unknown, which differs from equation (5.3) as the amplitude of the waves increases.

## 5.2 Regular perturbation method for $F_{SP} \ll 1$

In this section we shall apply a regular perturbation method to the nonlinear integral equation (3.29) assuming that $F_{SP} \ll 1$. Hence, we express $\delta(\xi)$ as a power series, namely

$$\delta(\xi) \sim F_{SP}^2\delta_1(\xi) + F_{SP}^4\delta_2(\xi) + O(F_{SP}^6), \tag{5.4}$$

where $O(F_{SP}^6)$ denotes terms of order $F_{SP}^6$. Thus, we write the function $\sin\delta(\xi)$ as

$$\begin{aligned}\sin\delta(\xi) &= \sin\left[F_{SP}^2\delta_1(\xi) + F_{SP}^4\delta_2(\xi) + O(F_{SP}^6)\right] \\ &\sim F_{SP}^2\delta_1(\xi) + F_{SP}^4\delta_2(\xi) + O(F_{SP}^6).\end{aligned} \tag{5.5}$$

We take the exponential of equation (3.29) to give

$$\left[\frac{(\xi-1)(\xi-\xi_B)}{\xi^2}\right]^{1/2}\exp\left[\frac{1}{\pi}\int_1^\infty \frac{\delta(\xi')}{\xi'-\xi}d\xi'\right] = \left[-\frac{3\mu^3}{\pi F_{SP}^2}\int_1^\xi \frac{\sin\delta(\xi')}{\xi'}d\xi'\right]^{1/3}. \tag{5.6}$$

Substituting asymptotic expansions (5.4) - (5.5) into the left-hand side of equation (5.6) yields

$$\begin{aligned}&\left[\frac{(\xi-1)(\xi-\xi_B)}{\xi^2}\right]^{1/2}\exp\left[\frac{F_{SP}^2}{\pi}\int_1^\infty \frac{\delta_1(\xi')}{\xi'-\xi}d\xi' + O(F_{SP}^4)\right] \\ = &\left[\frac{(\xi-1)(\xi-\xi_B)}{\xi^2}\right]^{1/2}\left[1 + \frac{F_{SP}^2}{\pi}\int_1^\infty \frac{\delta_1(\xi')}{\xi'-\xi}d\xi' + O(F_{SP}^4)\right],\end{aligned}$$

while the same substitution into the right-hand side yields, after using the binomial expansion,

$$\begin{aligned}
&\left[-\frac{3\mu^3}{\pi}\int_1^\xi \frac{\delta_1(\xi')}{\xi'}d\xi' - \frac{3\mu^3 F_{SP}^2}{\pi}\int_1^\xi \frac{\delta_2(\xi')}{\xi'}d\xi' + O(F_{SP}^4)\right]^{1/3} \\
&= \left[-\frac{3\mu^3}{\pi}\int_1^\xi \frac{\delta_1(\xi')}{\xi'}d\xi'\right]^{1/3}\left[1 + \frac{\frac{3\mu^3 F_{SP}^2}{\pi}\int_1^\xi \frac{\delta_2(\xi')}{\xi'}d\xi'}{\frac{3\mu^3}{\pi}\int_1^\xi \frac{\delta_1(\xi')}{\xi'}d\xi'} + O(F_{SP}^4)\right]^{1/3} \\
&= \left[-\frac{3\mu^3}{\pi}\int_0^\xi \frac{\delta_1(\xi')}{\xi'}d\xi'\right]^{1/3}\left[1 + \frac{\frac{\mu^3 F_{SP}^2}{\pi}\int_1^\xi \frac{\delta_2(\xi')}{\xi'}d\xi'}{\frac{3\mu^3}{\pi}\int_1^\xi \frac{\delta_1(\xi')}{\xi'}d\xi'} + O(F_{SP}^4)\right] \\
&= \left[-\frac{3\mu^3}{\pi}\int_1^\xi \frac{\delta_1(\xi')}{\xi'}d\xi'\right]^{1/3} + \frac{\frac{\mu^3 F_{SP}^2}{\pi}\int_1^\xi \frac{\delta_2(\xi')}{\xi'}d\xi'}{\left[\frac{3\mu^3}{\pi}\int_1^\xi \frac{\delta_1(\xi')}{\xi'}d\xi'\right]^{2/3}} + O(F_{SP}^4).
\end{aligned}$$

We take leading powers in the above expansions to obtain

$$-\frac{3\mu^3}{\pi}\int_1^\xi \frac{\delta_1(\xi')}{\xi'}d\xi' = \left[\frac{(\xi-1)(\xi-\xi_B)}{\xi^2}\right]^{3/2}, \tag{5.7}$$

and the terms of order $F_{SP}^2$ to give

$$\frac{\frac{\mu^3}{\pi}\int_1^\xi \frac{\delta_2(\xi')}{\xi'}d\xi'}{\left[\frac{3\mu^3}{\pi}\int_1^\xi \frac{\delta_1(\xi')}{\xi'}d\xi'\right]^{2/3}} = \left[\frac{(\xi-1)(\xi-\xi_B)}{\xi^2}\right]^{1/2}\frac{1}{\pi}\fint_1^\infty \frac{\delta_1(\xi')}{\xi'-\xi}d\xi'.$$

In light of the expression (5.7), this last equation can be rewritten as

$$-\mu^3\int_1^\xi \frac{\delta_2(\xi')}{\xi'}d\xi' = \left[\frac{(\xi-1)(\xi-\xi_B)}{\xi^2}\right]^{3/2}\fint_1^\infty \frac{\delta_1(\xi')}{\xi'-\xi}d\xi'. \tag{5.8}$$

Thus equation (5.7) gives us an equation for the leading order term $\delta_1$, and with this determined (5.8) is an equation for the correction term $\delta_2$. In principle, we could derive equations for higher terms in our expansion (5.4), however these would soon become increasingly complex and cumbersome, and impossible to solve analytically. Thus, we concentrate on solving for $\delta_1$ and $\delta_2$.

To solve for $\delta_1$ we differentiate equation (5.7) to give

$$-\frac{3\mu^3}{\pi}\frac{\delta_1(\xi)}{\xi} = \frac{d}{d\xi}\left[\frac{(\xi-1)(\xi-\xi_B)}{\xi^2}\right]^{3/2} = \frac{3}{2}\frac{\sqrt{(\xi-1)(\xi-\xi_B)}}{\xi^4}(\xi+\xi\xi_B-2\xi_B),$$

which after rearranging yields

$$\delta_1(\xi) = -\frac{\pi}{2\mu^3}\frac{\sqrt{(\xi-1)(\xi-\xi_B)}}{\xi^3}(\xi+\xi\xi_B-2\xi_B). \tag{5.9}$$

This expression was derived by Hocking and Forbes [7].

We now extend the result of Hocking and Forbes [7] by solving for $\delta_2$. To do this we need to substitute the expression for $\delta_1$ (5.9) into (5.8), which involves calculating

$$\fint_1^\infty \frac{\delta_1(\xi')}{\xi'-\xi}d\xi' = -\frac{\pi}{2\mu^3}\fint_1^\infty \frac{\sqrt{(\xi'-1)(\xi'-\xi_B)}(\xi'+\xi'\xi_B-2\xi_B)}{\xi'^3(\xi'-\xi)}\,d\xi'.$$

We calculate the above integral using the computer algebra manipulation package *Maple* to yield

$$\fint_1^\infty \frac{\sqrt{(\xi'-1)(\xi'-\xi_B)}(\xi'+\xi'\xi_B-2\xi_B)}{\xi'^3(\xi'-\xi)}\,d\xi' = \left[U\arctan(X)+W\ln|Y|-Z\right]_1^\infty, \qquad (5.10)$$

which has been simplified by introducing the five terms

$$U = -\frac{1}{4}\frac{1}{\xi^3\sqrt{(-\xi_B)}}\left(\xi^2+\xi^2\xi_B^2-8\xi\xi_B^2-8\xi\xi_B+6\xi^2\xi_B+8\xi_B^3\right), \qquad (5.11)$$

$$W = -\frac{1}{\xi}\sqrt{(\xi-1)(\xi-\xi_B)}(\xi+\xi\xi_B-2\xi_B), \qquad (5.12)$$

$$X = \frac{\xi'+\xi'\xi_B-2\xi_B}{2\sqrt{(-\xi_B)}\sqrt{(\xi'-1)(\xi'-\xi_B)}}, \qquad (5.13)$$

$$Y = \frac{-\xi'-\xi'\xi_B+2\xi_B-\xi'-\xi'}{\xi'-\xi}, \qquad (5.14)$$

$$Z = -\frac{1}{2}\frac{1}{\xi^2\xi'^2}\left(2\xi\xi_B-3\xi\xi_B\xi'-3\xi\xi'+4\xi'\xi_B\right)\sqrt{(\xi'-1)(\xi'-\xi_B)}. \qquad (5.15)$$

The limits are applied to the above expression to starting with (5.13), which yields

$$X\to\infty \quad \text{as} \quad \xi'\to 1^+, \quad \text{thus,} \quad \arctan(X)\to\frac{\pi}{2},$$

$$X\to\frac{1+\xi_B}{2\sqrt{-\xi_B}} \quad \text{as} \quad \xi'\to\infty, \quad \text{thus,} \quad \arctan(X)\to\arctan\left(\frac{1+\xi_B}{2\sqrt{-\xi_B}}\right)=\frac{\pi}{2}-2\arctan\sqrt{-\xi_B},$$

where the last result was rewritten with a simple trig identity. The limits are applied to equations (5.14)-(5.15) give

$$Y\to -1+\xi_B \quad \text{as} \quad \xi'\to 1^+, \quad \text{thus,} \quad \ln|Y|\to\ln|1-\xi_B|,$$

$$Y\to -1-\xi_B+2\xi+2\sqrt{(\xi-1)(\xi-\xi_B)} \quad \text{as} \quad \xi'\to\infty,$$

$$Z\to 0 \quad \text{as} \quad \xi'\to 1^+,$$

$$Z\to\frac{3}{2}\frac{\xi_B}{\xi}+\frac{3}{2\xi}-\frac{2\xi_B}{\xi^2} \quad \text{as} \quad \xi'\to\infty.$$

These results are substituted into expression (5.10) to yield

$$\fint_1^\infty \frac{\delta_1(\xi')}{\xi'-\xi}d\xi' = \frac{1}{2}\frac{1}{\xi^3\sqrt{(-\xi_B)}}\left(\xi^2+\xi^2\xi_B^2-8\xi\xi_B^2-8\xi\xi_B+6\xi^2\xi_B+8\xi_B^3\right)\arctan\sqrt{-\xi_B}...$$

$$-\frac{1}{\xi}\sqrt{(\xi-1)(\xi-\xi_B)}(\xi+\xi\xi_B-2\xi_B)\ln\left|\frac{-1-\xi_B+2\xi+2\sqrt{(\xi-1)(\xi-\xi_B)}}{1-\xi_B}\right|-\frac{3}{2}\frac{\xi_B}{\xi}+\frac{3}{2\xi}-\frac{2\xi_B}{\xi^2}. \tag{5.16}$$

Thus, we obtained an expression for $\delta_2$ by substituting (5.16) into equation (5.8), and differentiating the result in *Maple* to give

$$\begin{aligned}
\delta_2(\xi) &= -\frac{\xi}{\mu^3}\frac{d}{d\xi}\left(\left[\frac{(\xi-1)(\xi-\xi_B)}{\xi^2}\right]^{3/2}\fint_1^\infty\frac{\delta_1(\xi')}{\xi'-\xi}d\xi'\right)\\
&= \frac{\pi}{8\mu^6}\frac{\sqrt{(\xi-1)(\xi-\xi_B)}}{\xi^5}\Bigg\{\Bigg[(2\xi_B^2+12\xi_B+2)\xi^4-(\xi_B+1)(5\xi_B^2+62\xi_B+5)\xi^3\\
&\quad+16\xi_B(4\xi_B^2+13\xi_B+4)\xi^2-152\xi_B^2(\xi_B+1)\xi+96\xi_B^2\Bigg]\frac{\arctan\sqrt{-\xi_B}}{\xi\sqrt{-\xi_B}}\\
&\quad+10(1+\xi_B)\xi^3-(19\xi_B^2+62\xi_B+19)\xi^2+64\xi_B(\xi_B+1)-48\xi_B^2\\
&\quad-\frac{4\sqrt{(\xi-\xi_B)(\xi-1)}}{\xi}\Bigg[(\xi_B+1)\xi^3-(3+\xi_B)(3\xi_B+1)\xi^2+13\xi_B(\xi_B+1)\xi-12\xi_B^2\Bigg]\\
&\quad\times\log\left(\frac{2\xi-1-\xi_B+2\sqrt{(\xi-1)(\xi-\xi_B)}}{1-\xi_B}\right)\Bigg\}.
\end{aligned} \tag{5.17}$$

Note that if the source is situated on on the channel floor then $\xi_B = 0$. By taking the limit $\xi_B \to 0^-$ above we find that (5.9) and (5.17) reduce to the rather simple expressions

$$\delta_1(\xi) = -\frac{\pi}{2\mu^3}\frac{\sqrt{(\xi-1)\xi}}{\xi^2}, \tag{5.18}$$

$$\delta_2(\xi) = \frac{\pi}{2\mu^6}\left(\frac{3\sqrt{\xi-1}}{\xi^{5/2}}(\xi-2)-\frac{(\xi-1)(\xi-3)}{\xi^3}\ln\left[2\xi-1+2\sqrt{\xi(\xi-1)}\right]\right). \tag{5.19}$$

These expressions are substituted into the original power series (5.4) to a asymptotic expression for $\delta(\xi)$ that serves as a good initial guess to our numerical scheme.

## 5.3 Asymptotic description which includes waves

The regular perturbation method outlined in section 5.2 predicts a horizontal free surface in the far stream. However, numerical results in chapter 6.2 (see figure 6.5) suggest that a train of waves does exist on the free surface, whose amplitude is exponentially small as $F_{SP}$

approaches zero. This would explain why our regular perturbation method does not capture the waves since $\exp(-\beta/F_{SP}^2)$ cannot be written as a power series in $F_{SP}^2$ [12]. Hence, this implies that the free surface waves are *beyond all orders*, or equivalently, they are smaller than every term in the regular perturbation series

$$\delta(\xi) = \sum_{n=1}^{\infty} F_{SP}^{2n} \delta_n(\xi). \tag{5.20}$$

Thus, in order to describe the free surface completely, including waves, in the limit $F_{SP} \to 0$, we must employ *exponential asymptotics*. Unfortunately, this is a highly complex and rigorous theory that is beyond the scope of an honours project. In lieu of this we briefly outline how this method could be employed.

Firstly, it should be noted that in principle it is possible to derive any number of terms in a series like (5.20), but in practice any more than two terms would become nearly impossible, even if employing symbolic packages like *Maple*. Typically, for a fixed value of $F_{SP}$ such a series would be divergent [12]. Furthermore, the error will likely decrease as more terms are included up to a certain point, but then increase without bound. Thus, it should be possible to optimally truncate the series in order to minimized the error. This optimally truncated asymptotic series is sometimes referred to as *superasymptotic* [12].

The crucial point here is that the error in a superasymptotic series is typically of the order $\exp(-\beta/\epsilon)$, where $\epsilon$ is a small parameter (in our case $\epsilon = F_{SP}^2$). These exponentially small terms form part of an *subdominant exponential*, and are hidden from normal view, but are "switched on" across a Stokes' line. This behaviour is closely related to Stokes' phenomena, which states that a single valued analytic function may have a different asymptotic expansion in different sections of the complex plane [11].

We mention that exponentially small capillary waves (due to surface tension but not gravity) have been successfully described using exponential asymptotics by Chapman and Vanden-Broeck [23] by first deriving a Nekrasov type integral equation (analogous to equation (3.29)). However, our type of problem has not been studied with asymptotic exponentials hence this remains a goal for future research.

# Chapter 6

# Presentation of Results

In this chapter we shall present a number of typical numerical and asymptotic results for varying $F_{SP}$ values and discuss their solution characteristics. We shall examine a numerical solution with waves and make a comparison between different values of $N$ and $\phi_N$ in order to argue that our chosen parameter values are suitable for our calculations. We shall compare the numerical and asymptotic solutions and outline the $F_{SP}$ range where they agree and where the asymptotic solution begins to break down. Finally, we shall analyze the behaviour of wave amplitude and wavelength for small values of $F_B$, recalling that $F_B$ is related to $F_{SP}$ by the expression

$$F_B = \frac{F_{SP}}{\mu^{3/3}}.$$

For an example, we have chosen to calculate solutions for a source located on the channel floor which corresponds to $\xi_B = 0$. Interestingly, this is also equivalent to two-dimensional problem of flow past a ship stern (see section 7.2.1) for the limit $H \to 0$.

## 6.1 Effects of numerical scheme parameters

We wish to use the most appropriate $\phi_N$ and $N$ parameter values in order to gain a solution with a reasonable degree of numerical accuracy. We have chosen $\phi_N = 8$ and $N = 800$, and presented a typical solution $F_{SP} = 0.4$ in figure 6.2, which shows a train of waves present upstream on the free surface. In order to justify this approximation for infinity, we present a second solution of $F_{SP} = 0.4$ with $\phi_N = 16$. In an attempt to counter the truncation errors of the coarser mesh for the $\phi_N = 16$ solution, the number of points is doubled to yield $N = 1600$,

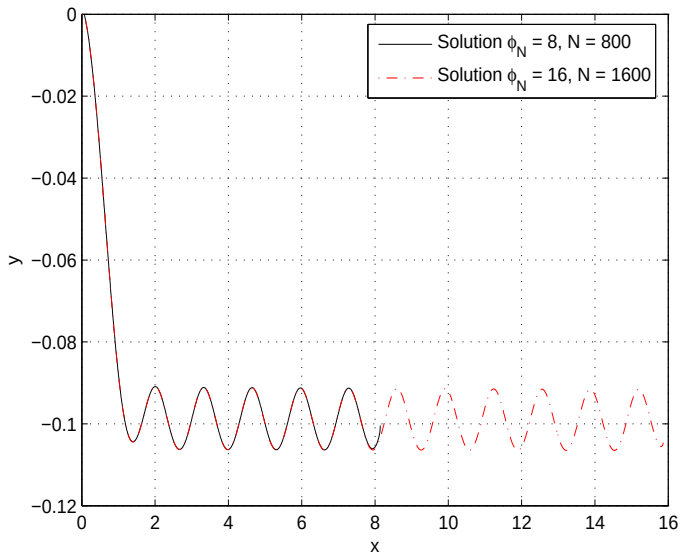


Figure 6.1: A comparison of free surface profiles to observe the effect of different approximations for infinity. $F_{SP} = 0.4$.

which ensures that the $\Delta\phi$ is the same value for both solutions.

The plot shows the two solutions agreeing remarkably well. The $\phi_N = 8$ solution is almost identical to the $\phi_N = 16$ solution. Seemingly, the larger $\phi_N$ value has no observable advantage and thus, we shall assume that $\phi_N = 8$ is a good approximation for infinity in our system.

Next we compare the solutions for $F_{SP} = 0.4$ when $N = 400$, $N = 800$ and $N = 1600$ in order to see what effect increasing the number of mesh points has on the solution. The three solutions agree with each other for low values of $x$, particularly before the first trough. However, the solutions begin to differ with an increase in $x$. Naturally, the $N = 400$ solution differs more than the $N = 800$ solution in comparison to the $N = 1600$ solution. It is assumed that $N = 1600$ solution is more accurate. However, it should be noted that when too many mesh points are used round-off errors become significant, thus reducing the overall accuracy of the system [18]. Although, it is not certain in which region of $N$ this problem manifests itself.

An important consideration, other than numerical accuracy, is the pragmatic concern of computation time. To give a rough measurement of computation time, the majority of these calculations were performed on a 1.3 GHz machine, which calculated the solution of a typical system ($F_{SP} = 0.35$, $\phi_N = 8$ and $N = 800$) in 113 minutes with an average of five to six

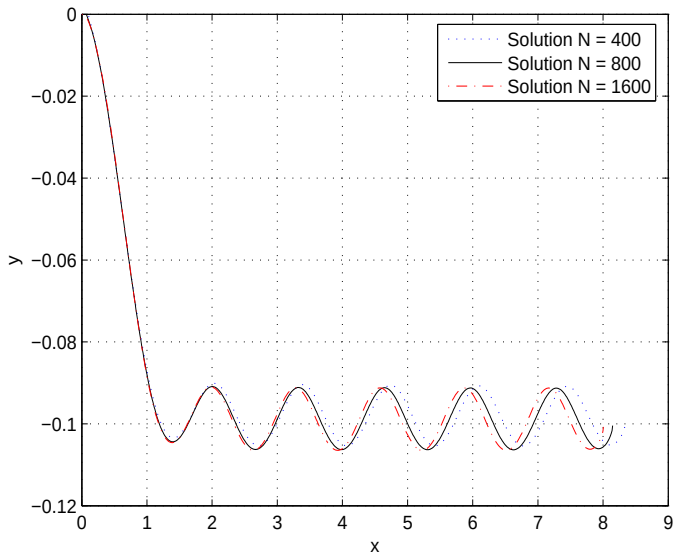


Figure 6.2: The effect on the numerical solution when the number of mesh points is varied. $F_{SP} = 0.4$, $F_B = 0.4677$ and $\mu = 0.9009$.

iterations.

Intuitively, when the mesh becomes finer the numerical scheme produces more accurate results. This advantageous increase in accuracy is countered by the obvious increase in the number of equations that need to be solved. Thus, the task of choosing the $N$ value, becomes a trade off between accuracy and computation time.

In conclusion, we found that $\phi_N = 8$ is a good approximation for infinity while $N = 800$ is very reasonable number of points and that increasing this value did not have a significant advantage when computation time was taken under consideration. Henceforth, we shall use the parameters $\phi_N = 8$ and $N = 800$ in all the ensuing solutions presented here unless stated otherwise.

## 6.2 Comparison of numerical and asymptotic solutions

Our asymptotic scheme, which we derived in chapter 5, is limited to the regime of low values of $F_{SP}$ and is incapable of producing solutions which possess waves on the free surface. We present a comparison of the numerical and asymptotic solutions.

The plots of the free surface profile and the angle of the free surface, $\delta$ in figures 6.3 -

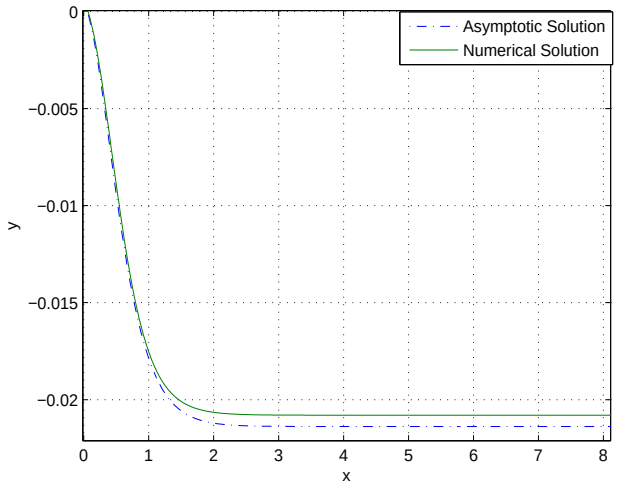


Figure 6.3: Comparison of asymptotic and numerical free surface profiles for $F_{SP} = 0.2$.

6.4 show that the asymptotic and numerical solutions are in close agreement for $F_{SP} = 0.2$. Although there are exponentially small waves present on the free surface of the numerical solution, which we discuss in the next section, the profile is virtually flat for this $F_{SP}$ value. Hence, the asymptotic approach serves as a good solution and an excellent initial guess for the numerical solution.

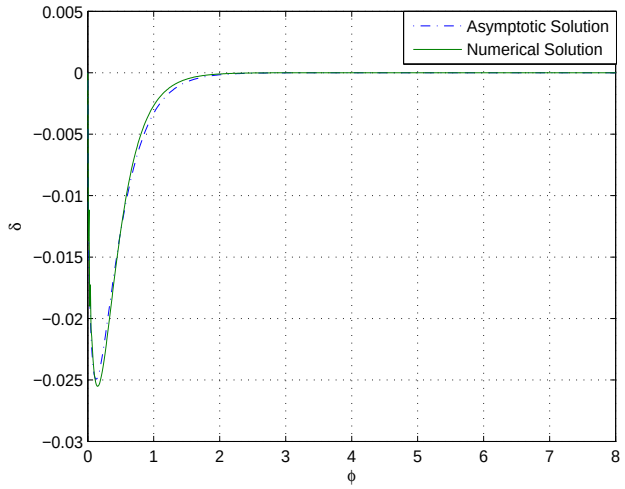


Figure 6.4: Comparison of asymptotic and numerical $\delta$ solutions for $F_{SP} = 0.2$.

In figure 6.5 a similar plot of the asymptotic and numerical solutions for $F_{SP} = 0.45$ shows that they are not in agreement, which is to be expected as the asymptotic scheme becomes

more inaccurate as $F_{SP}$ increases. In particular, there are sizeable waves present on the free surface while, as previously noted, our asymptotic solution is unable to produce a solution with waves.

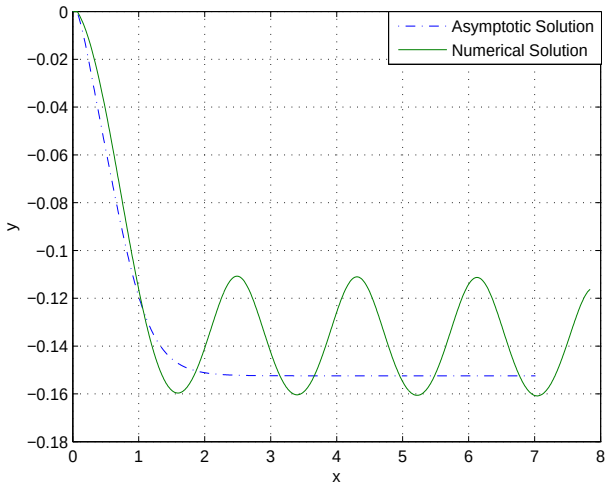


Figure 6.5: The asymptotic solutions breaks down for $F_{SP} = 0.45$.

Near the stagnation point, the plots of asymptotic and numerical $\delta$ agree with each other. However, as the asymptotic $\delta$ approaches zero in the far field (the free surface plateaus), the numerical $\delta$ continues to oscillate above and below zero corresponding to sizeable waves on the free surface. The asymptotic solution offers a reasonable $\delta$ guess for smaller waves. However, guesses such as $\delta$ solutions for smaller $F_{SP}$, should be considered instead of asymptotic $\delta$ solutions when dealing with larger $F_{SP}$ values.

## 6.3 Wave behaviour

We wish to shed light on the behaviour of the train of waves present on the free surface profile. In particular, we wish to analyse the variation of wave amplitude, $A$ and wavelength $\lambda$ with respect to $F_B$.

Mekias and Vanden-Broeck in their original paper [8] observed for small values of $F_B$ an apparent linear relationship existing between $-1/F_B^2$ and $\ln(A)$. By plotting $\ln(A)$ versus $-1/F_B^2$, we observed a similar linear relationship in figure 6.7, which suggests

$$A = \alpha e^{-\beta/F_B^2} \quad \text{as} \quad F_B \to 0, \tag{6.1}$$

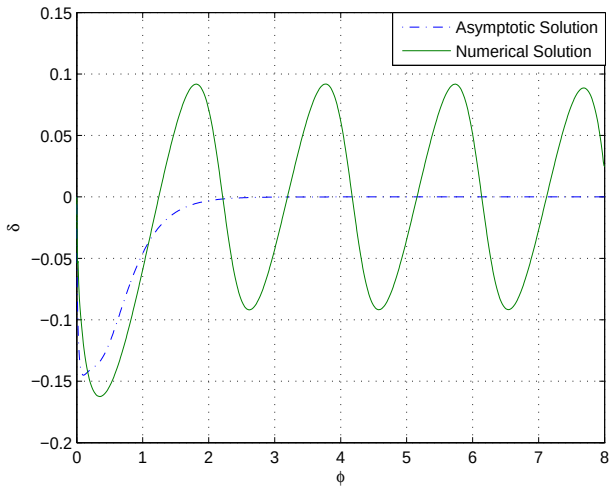


Figure 6.6: Asymptotic solution is unable to predict waves for $F_{SP} = 0.45$

where $\alpha$ and $\beta$ are constants of the individual system and are, according to Mekias and Vanden-Broeck [8], related to the location of the source.

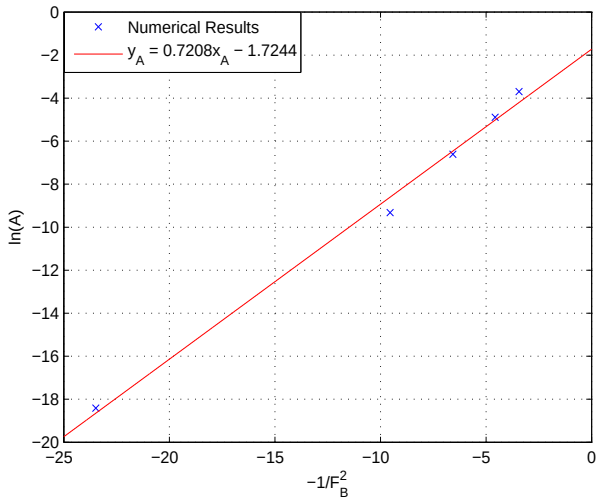


Figure 6.7: A linear fit of the numerical results that suggest $A$ decreases exponentially.

Since the amplitude of the free surface waves decreases rapidly due to their exponential nature, waves are barely visible for smaller values of $F_B$, and hence the profiles appear flat. Vanden-Broeck suggests in his reconciliation work [9] that this may be the reason why waves were not visible in the results of Hocking and Forbes [7]. We tend to agree with this conclusion since our results show seemingly flat profiles for values such as $F_B = 0.2064$.

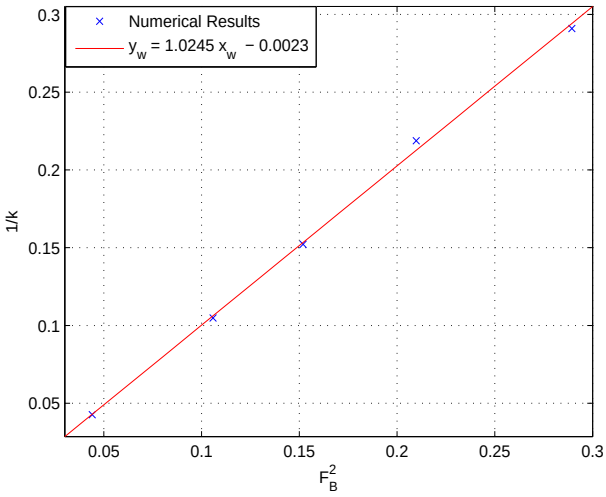


Figure 6.8: A fitted line with an almost unity gradient suggesting an exact expression for $k$.

Our results demonstrate that free surface waves exhibit a periodic behaviour. In order to illuminate this periodic nature, we introduce the wave number, defined as $k = 2\pi/\lambda$. For the regime of $0.2 \leq F_{SP} \leq 0.45$, we plot $1/k$ versus $F_B^2$ and obtain an elegant linear relationship. The corresponding fitted-line has a gradient of almost unity, which strongly suggests

$$\frac{1}{k} = \frac{\lambda}{2\pi} = F_B^2 \quad \text{as} \quad F_B \to 0. \tag{6.2}$$

The equivalent relationship based on linear wave theory is

$$F_B^2 = \frac{1}{k}\tanh(k), \tag{6.3}$$

which reduces to our empirical expression (6.2) as we approach the limit

$$\tanh(k) \to 1 \quad \text{as} \quad \frac{1}{k} \to 0.$$

Thus, this relationship is a reliable vindication of our results and overall solution method.

Finally, our results in figures (6.9) and (6.10) reveal that the general form of the waves continues to change as $F_{SP}$ increases. The waves are no longer sinusoidal in shape, but begin to have narrow crests and broad troughs. For larger Froude numbers the waves will approach the Stokes' limiting configuration with 120-degree crests [15]. However, the number of points needed for these types of calculations is more than feasible.

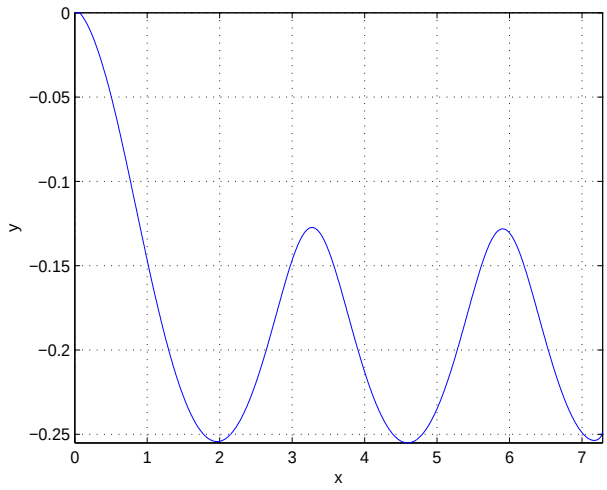


Figure 6.9: Narrower crests and broader troughs for $F_{SP} = 0.5$.

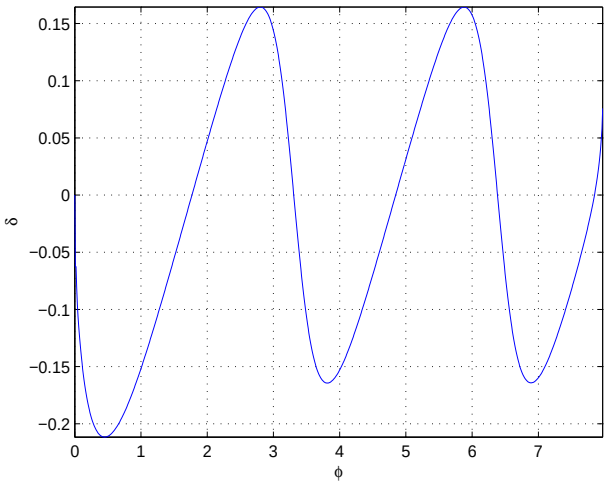


Figure 6.10: The free surface angle, $\delta$ becoming skewed for $F_{SP} = 0.5$.

# Chapter 7

# Conclusion and Discussion

## 7.1 Summary of project

In this project we have presented a lucid formulation of a free surface problem with flow due to a submerged source in a channel of finite depth. We have clearly declared all our assumptions and, correspondingly, derived all the necessary governing equation and boundary conditions. In the process, we have rectified and clarified any errors and misconceptions.

We have employed complex variable theory in a similar manner as others have done before us to solve free surface problems [7, 9, 10]. Using conformal mapping and Cauchy's integral theorem, we have obtain a singular nonlinear integral equation. This integral equation has been solved by representing it with trapezoidal scheme and solving the resulting set of nonlinear equations with the *fsolve* function and in the process we have carefully dealt with all the singularities .

We have extended the work of Hocking and Forbes [7] by deriving a second order asymptotic solution for $\delta(\xi)$, which is valid for the regime of small $F_B$, and as such, the asymptotic results have agreed well with the numerical results in this regime. We have discussed how exponential asymptotics could be used to derive a more accurate analytic solution that describes waves on the fee surface.

We have obtained results showing waves of significant amplitude on the free surface, which is in agreement of previous solutions [7, 9, 10]. We have studied the behaviour of the free surface waves in relation to the $F_B$ value and have verified and obtained a number of relationships, which agree with previous observations [9] and linear wave theory [15]. Thus,

we have vindicated our results and solution methods with these empirical observations and relationships.

## 7.2 Related free surface problems

It happens that the problem of flow due to a line source is closely related to a number of other free surface problems, such as the flow past the stern of a ship, and the flow under a sluice gate. As a result, the solution methods employed here may be adapted for these related problems. We briefly discuss the problems here.

### 7.2.1 Flow past the stern of a ship

Evidently, when ships travel through water they create waves. This wave creation is generally unwanted as it creates drag, which results in more energy being spent to propel the ship. For naval vessels, waves are unwanted for an additional reason as waves leave a "foot print" thus allowing it to be detected by an enemy. Thus, ships should be designed in order to minimize wave generation and hence drag.

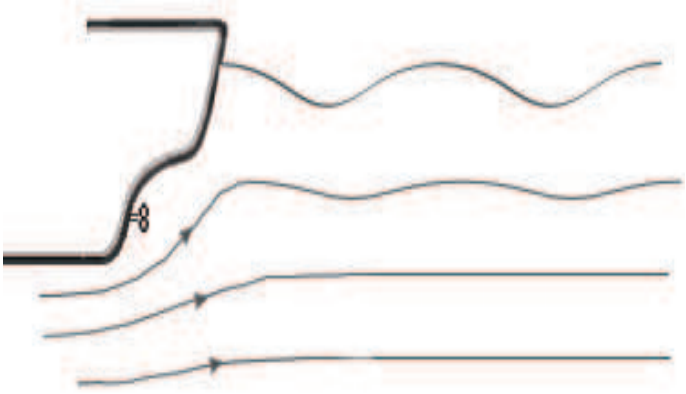

Figure 7.1: Flow past a regular ship stern.

In two dimensions we can study the flow past a stern of a ship by assuming that the stern is semi-infinite, as in figure 7 of Tuck's [3] (reproduced here as figure 7.1). Numerous problems of this nature have been analyzed numerically [3, 24, 25, 26, 27]. For example, various stern shapes have been tried in order to minimize the amplitude of the waves they create, with

varying success. These studies have been numerical in nature, with no precise understanding of the exact relationship between wave amplitude and stern shape.

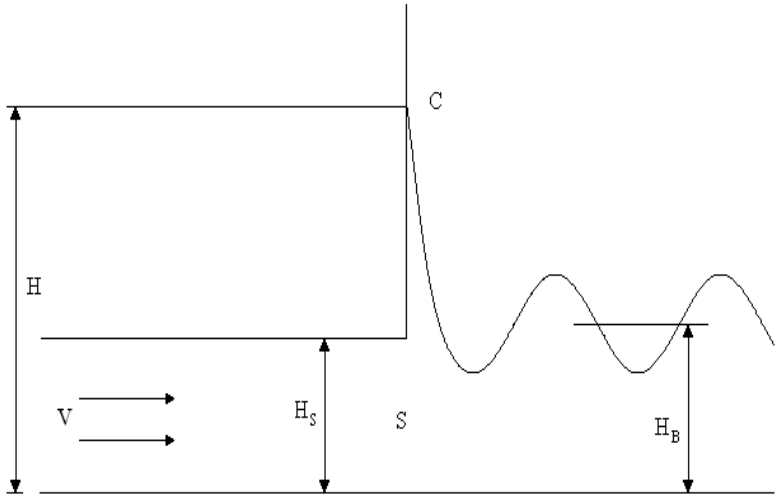


Figure 7.2: Flow past a rectangular ship stern.

In order to see how similar the problem presented in this thesis is we consider the simple case when the ship stern is rectangular in shape as indicated in figure 7.2. We scale the variables to yield

$$x = \frac{\bar{x}}{H}, \quad y = \frac{\bar{y}}{H}, \quad \mu = \frac{H_B}{H}, \quad \gamma = \frac{H_S}{H},$$

and scale the velocities with respect to $V\lambda$, so

$$q \to \frac{1}{\lambda} \quad \text{as} \quad x \to -\infty.$$

The Bernoulli equation, which is satisfied anywhere along the free surface, becomes

$$\frac{1}{2}\left(\frac{m^2}{gH^3}\right) q^2 + y = 0.$$

We reintroduce the complex potential $f(z) = \phi(x, y) + i\psi(x, y)$, and expressed the complex velocity as

$$\frac{df}{dz} = w = u - iv.$$

The problem is mapped to the $f$-plane, then to the $\zeta$-plane. The complex velocity is now expressed as

$$w = \frac{1}{\mu} e^{-i\Omega(\zeta)},$$

where $\Omega(\zeta) = \delta(\zeta) + i\tau(\zeta)$. The flow conditions of the physical problem give the flow angles

$$\delta(\xi) = \begin{cases} 0 & \text{if } -\infty < \xi < \xi_S, \\ \pi/2 & \text{if } \xi_S < \xi < 1, \\ \text{unknown} & \text{if } \xi > 1. \end{cases}$$

The Bernoulli equation is recast and manipulated to become

$$\tau(\xi) = \frac{1}{3} \ln \left[ -\frac{3\mu^3}{\pi F_{SP}^2} \int_1^{\xi} \frac{\sin \delta(\xi')}{\xi'} d\xi' \right].$$

We invoke the Cauchy integral formula and use the aforementioned $\delta(\xi)$ values to obtain the integral equation

$$\tau(\xi) = \frac{1}{2} \ln \frac{(\xi - 1)}{(\xi - \xi_B)} + \frac{1}{\pi} \int_1^{\infty} \frac{\delta(\xi')}{\xi' - \xi} d\xi',$$

which is combined with the Bernoulli equation to yield

$$\frac{1}{2} \ln \frac{(\xi - 1)}{(\xi - \xi_B)} + \frac{1}{\pi} \int_1^{\infty} \frac{\delta(\xi')}{\xi' - \xi} d\xi' - \frac{1}{3} \ln \left[ -\frac{3\mu^3}{\pi F_{SP}^2} \int_1^{\xi} \frac{\sin \delta(\xi')}{\xi'} d\xi' \right] = 0.$$

This integral equation is almost identical to our integral equation (3.29), and as such, can be solved with an approach similar to ours.

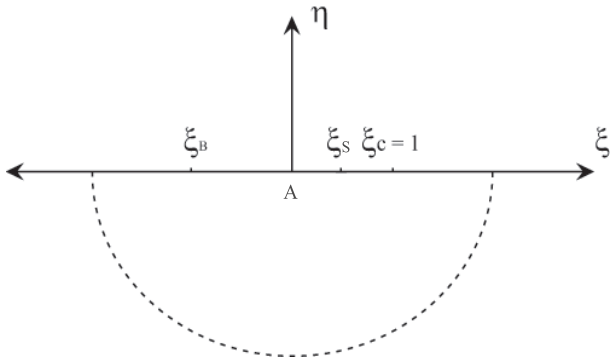


Figure 7.3: The lower half of the $\zeta$-plane.

### 7.2.2 Flow under a sluice gate

The flow under a sluice gate is a classical problem in applied mathematics, studied by [4, 28], and many others. This problem is similar to the flow due to a source and flow past a stern because of the stagnation point (see point B on figure 7.4). This problem is more difficult to

solve due to the presence of the two free surfaces, however, conformal mapping can be used similarly to give an integral equation analogous to ours. We omit the details, but instead refer the reader to [4].

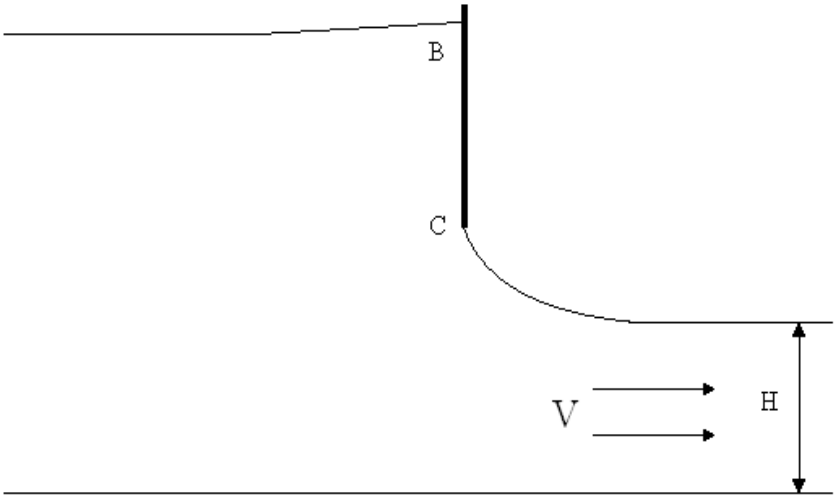


Figure 7.4: Flow under a sluice gate with two free surfaces.

## 7.3 Further research

### 7.3.1 Exponential Asymptotics

Since our asymptotic analysis is apparently incapable of capturing the exponentially small terms that produce the free surface waves, it seems the terms are beyond all orders. However, it may be possible to shed more light on on this area by employing exponential asymptotics in order to derive an asymptotic expansion that captures the free surface waves for small Froude numbers. This would be indeed an exciting and difficult task for future research.

### 7.3.2 Flow due to a sink

If it is possible to show with exponential asymptotics that a train of waves, albeit exponentially small, always exist on the free surface then, by the Sommerfield radiation condition, we can infer that the flow field is due to a line source, and cannot be used to describe flow due to a line sink. Thus, the question remains, what is the flow configuration if there is a link sink, and not a line source, present? As mentioned in section 1.2, this is an important question in regards

to fluid withdrawal of various reservoirs. In order to answer question, further research is required, particularly for the case of Froude numbers less than unity, as this problem remains open

### 7.3.3 Stern flows

We have illustrated in section 7.2.1 how our problem is very similar to that of flow past a ship stern in two dimensions. Hence, we expect for this case that exponentially small waves would exist on the free surface for small Froude numbers. Similarly, these waves could possibly be described with the use of exponential asymptotics although this would be an arduous task. However, an exciting prospect of employing exponential asymptotics is the possibility of deriving analytical results that relate the shape of stern and the amplitude of the waves with the goal of designing an optimally shaped stern. This problem, along with the others discussed, remains open for future endeavours.

# Appendix A

# Numerical code

## A.1 *froudesolve.m*

```
%Main Program
%Makes asymptotic initial guess, solves equations for delta (hock.m),
%calculates tau, calculates x and y for free surface, plots results
clear all; close all; t1=cputime; load nasymphi8Fs04; Fsp=0.4;
zb=0; n=100;
%Setting up the zeta values
phimax=12; phi=linspace(0,phimax,n); z=exp(pi*phi); zmax=z(end);
%Initial Guess
mu=1/3+2/3*cos(1/3*acos(1-27/4*Fsp^2));
guess=Fsp^2*(-pi/2/mu^3).*sqrt((z-1).*(z-zb))./z.^3.*(z+zb*(z-2));
guess(1)=mu;%mu guess

%fslove
options=optimset('Display','iter');   % Option to display output
%Minimising equations
guess= fsolve(@froude,guess,options); %Make sure the parameters match
%Retrieve calculated values
mu=guess(1); ndelta=[0 guess(2:end)];
```

```
%Calculate tau values
tau=[]; const=-3*mu^3/Fsp^2; for j=2:n
    tau(j)=(1/3)*log((const*trapezoid(phi(1:j),sin(ndelta(1:j)))));
end
tau=[0 tau]; %Zero is for adjusting length
%Calculate x and y
x=[];y=[];x(1)=0;y(1)=0;y(2)=0; j=2;
%Integrand before the singularity
fL=(ndelta(1:j-1)-ndelta(j))./(exp(pi*phi(1:j-1))-exp(pi*phi(j)))...
    .*exp(pi*phi(1:j-1));
%Integrand after the singularity
fU=(ndelta(j+1:end)-ndelta(j))./(exp(pi*phi(j+1:end))-exp(pi*phi(j)))...
    .*exp(pi*phi(j+1:end));
%Compute integrand at singularity
dd=(ndelta(j)-ndelta(j-1))/(phi(j)-phi(j-1))/pi;
%Complete integrand
fI=[fL dd fU];
%Calculate integral
xI=trapezoid(phi,fI);
%Log term from avoiding the singularity
expx=xI+(ndelta(j)/pi)*log(abs((zmax-z(j))/(z(j)-1)));
x(2)=(2*mu/pi)*sqrt(exp(phi(2))-1)*exp(-expx); for j=3:n
    funx=exp(-tau(2:j)).*cos(ndelta(2:j))+x(2);
    x(j)=mu*trapezoid(phi(2:j),funx)+x(2);
    funy=exp(-tau(2:j)).*sin(ndelta(2:j));
    y(j)=mu*trapezoid(phi(2:j),funy);
end
%Plot results
%Plot free surface profile
totaltime=cputime-t1 plot(x,y,ax2,ay2);grid; axis tight;
legend('Numerical Solution', 'Asymptotic Solution'); figure;
```

```
%Plot delta
plot(x,ndelta, ax2,adelta2); grid;legend('Numerical Delta',
'Asymptotic Delta'); save newnum1200phi12Fs055.mat x y ndelta phi
Fsp mu; mu Fb=Fsp/mu^1.5
```

## A.2 *froude.m*

```
%Equation definition file
function y = froude(guess)
%y is the function to be minimized
%guess is the input vector
%j reprsents equation to use, i represnts variable to perturb
Fsp=0.4; zb=0;
n=length(guess); %Number of equations
mu=guess(1);%mu guess
%Create delta vector
d=[0 guess(2:end)];
%Setting up the zeta and alpha values
phimax=12; phi=linspace(0,phimax,n); z=exp(pi*phi); zmax=z(n); for
j=1:n
    %Calculate the mu value
    if j==1
        nz=500;
        theta=linspace(-pi/2,pi/2,nz);
        zeta=0.5*(sin(theta)+1);
        %Calculate exponential tau
        fun=[];
        for k=1:nz
            if k==nz
                %Avoiding Singularity
```

```
            %Improper Integral
            pv=-1*trapezoid(phi(2:n),d(2:n)./...
                (exp(pi*phi(2:n))-zeta(k)).*exp(pi*phi(2:n)));
            fun(nz)=exp(pv);
        else
            %Improper Integral
            pv=-1*trapezoid(phi,d./(exp(pi*phi)-zeta(k)).*exp(pi*phi));
            fun(k)=exp(pv);
        end
    end
    y(j)=1-(mu/pi)*trapezoid(theta,fun);

elseif j==n
    %3 point extrapolation
    dend=3*d(n-1)-3*d(n-2)+d(n-3);  %Extrapolated value
    y(j)=dend-d(n);



else
    %Setting up the y equations
    %First term in equation
    y1=0.5*log(((exp(pi*phi(j))-zb)*(exp(pi*phi(j))-1)...
        /exp(2*pi*phi(j))));

    %Second Term - involes the improper PV integral
    %Integrand before the singularity
    f2L=(d(1:j-1)-d(j))./(exp(pi*phi(1:j-1))-exp(pi*phi(j)))...
        .*exp(pi*phi(1:j-1));
    %Integrand after the singularity
    f2U=(d(j+1:end)-d(j))./(exp(pi*phi(j+1:end))-exp(pi*phi(j)))...
        .*exp(pi*phi(j+1:end));
```

```
        %Compute integrand at singularity
        dd=(d(j)-d(j-1))/(phi(j)-phi(j-1))/pi;

        %Complete integrand
        f2I=[f2L dd f2U];
        %Calculate integral
        y2I=trapezoid(phi(1:end),f2I(1:end));
        %Log term from avoiding the singularity
        y2=y2I+(d(j)/pi)*log(abs((zmax-z(j))/(z(j)-1)));

        %Third term - involves integral
        const=-3*mu^3/Fsp^2;
        y3=(-1/3)*log(abs(const*trapezoid(phi(1:j),sin(d(1:j)))));
        y(j)=y1+y2+y3;
    end
end
```

## A.3 *trapezoid.m*

```
%Trapezoid Scheme
function z = trapezoid(x,y) nx=length(x); ny=length(y); if nx==ny
    if nx==1
        z=0;
    else
        z = diff(x).* (y(1:ny-1) + y(2:ny))/2; %Area for each trapezoid
        z=sum(z);   %Sum trapezoids
    end
else
    'Vector lengths do not match'
end
```

# Bibliography


[1] G.C. Hocking. Supercritical withdrawal from a two-layer fluid through a line source. *Journal of Fluid Mechanics*, 297:37–47, March 1995.

[2] G.C. Hocking and L.K. Forbes. Withdrawal from a two-later invisid fluid in a duct. *Journal of Fluid Mechanics*, 361:275–296, December 1997.

[3] E.O. Tuck. Ship-hydrodynamics free-surface problems without waves. *Journal of Ship Research*, 35(4):277–287, 1991.

[4] J.-M. Vanden-Broeck. Numerical calculations of the free-surface flow under a sluice gate. *Journal of Fluid Mechanics*, (330):339–347, 1997.

[5] J.J. Stoker. *Water Waves: The Mathematical Theory with Applications*. Interscience Publishers Inc., 1st edition, 1957.

[6] L. Debnath. *Nonlinear Water Waves*. Academic Press, 1st edition edition, 1994.

[7] G.C. Hocking and L.K. Forbes. Subcritical free-surface flow caused by a line source in a fluid of finite depth. *Journal of Engineering Mathematics*, (26):455–466, 1992.

[8] H. Mekias and J.-M. Vanden Broeck. Subcritical flow with a stagnation point due to a soruce beneath a free surface. *Phys. Fluids A*, (11):2652–2658, 1991.

[9] J.-M. Vanden-Broeck. Waves generated by a source below a free surface in water of finite depth. *Journal of Engineering Mathematics*, (30):603–609, 1996.

[10] G.C. Hocking and L.K. Forbes. Withdrawal from a fluid of finite depth through a line sink, including surface-tension effects. *Journal of Engineering Mathematics*, (38):91–100, 2000.

[11] L.M. Milne Thomson. *Theoretical Hydrodynamics*. MacMillan, 5th edition, 1974.

[12] J.P. Boyd. The devil's invention: asymptotic, superasymptotic and hyperasymptotic series. *Acta Applicandae Mathematicae: An International Survey Journal on Applying Mathematics and Mathematical Applications*, 56:1–98, March 1999.

[13] G.K. Batchelor. *An Introduction to Fluid Dynamics*. Cambridge University Press, 1st edition, 1967.

[14] M. L. Boas. *Mathematical Methods in the Physical Sciences*. Wiley, 2nd edition, 1983.

[15] M. Rahaman. *Water Waves: Relating Modern Theory to Advanced Engineering Practice*. Oxford Science Publications, 1st edition, 1995.

[16] G.B. Arfken and H. J. Weber. *Mathematical Methods for Physicists*. Academic Press, 4th edition, 1995.

[17] J.V. Wehausen and E.V. Laitone. Surface waves. In *Handbuch der Physik*.

[18] W. T. Vetterling W.H. Press, S.A. Teukolsky and B. P. Flannery. *Numerical Recipes in C*. Cambridge Press, 2nd edition, 1997.

[19] G.C. Hocking and J.-M. Vanden-Broeck. Withdrawal of a fluid of finite depth through a line sink with a cusp in the free surface. *Computers and Fluids*, 27:797–806, December.

[20] M.A. Branch T. Coleman and A. Grace. *Optimization Toolbox User's Guide*. The Maths Works Inc., third edition edition, 1999.

[21] J. J. Moré. *Numerical Analysis*. Springer Verlag, 1st edition, 1977.

[22] M. Abramowitz and I. Stegun. *Handbook of Mathematical Functions*. Dover, 1970.

[23] S.J. Chapman and J.-M. Vanden-Broeck. Exponential asymptotics and capillary waves. *SIAM Journal of Applied Mathematics*, 62:1872–1898, 2002.

[24] M.A.D. Madurasinghe. Splashless ship bows with stagnant attachment. *Journal of Ship Research*, 32:194–202, 1988.

[25] D.E. Farrow and E.O. Tuck. Further studies of stern wakemaking. *Journal of the Australian Mathematical Society, Series B*, 36:424–437, 1995.

[26] S.W. McCue and L.K. Forbes. Bow and stern flows with constant vorticity. *Journal of Fluid Mechanics*, 399:277–300, 1999.

[27] J.-M. Vanden-Broeck and E.O. Tuck. Computation of near-bow or stern flows, using series expansion in the froude number. *Proceedings of the 2nd International Conference of Numerical Ship Hydrodynamics, Berkeley*, pages 371–381, 1977.

[28] D.D. Fangmeier and T.S. Strelkoff. Solution for gravity flow under a sluice gate. *Journal of the Engineering Mechanics Division ASCE*, 94:153–176, 1968.

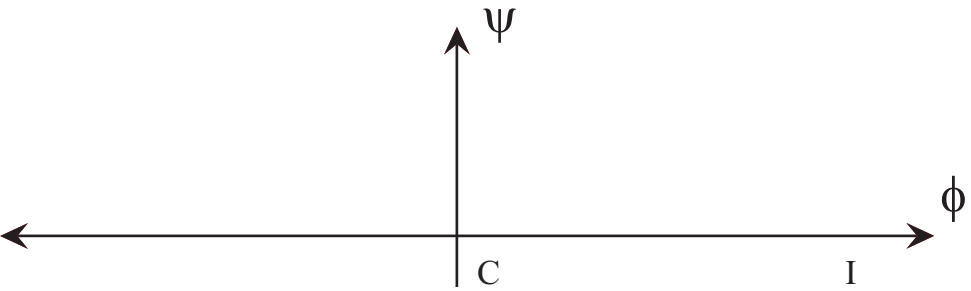
ψ
ϕ
C
I

S

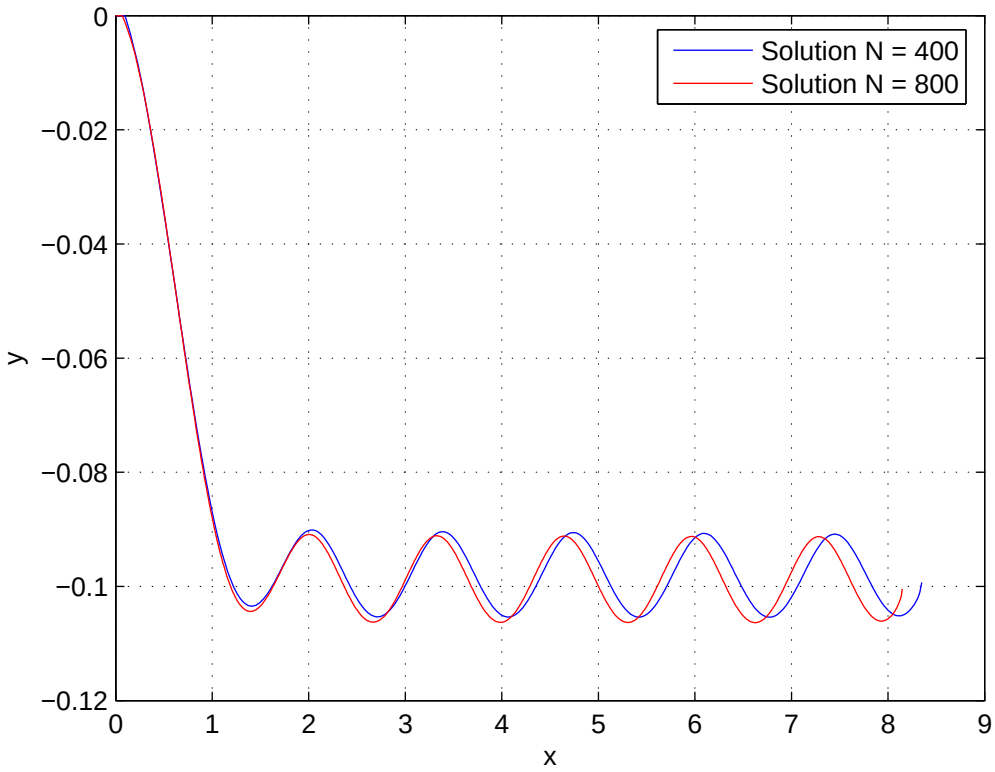
Solution N = 400
Solution N = 800
y
x
0
−0.02
−0.04
−0.06
−0.08
−0.1
−0.12
0
1
2
3
4
5
6
7
8
9

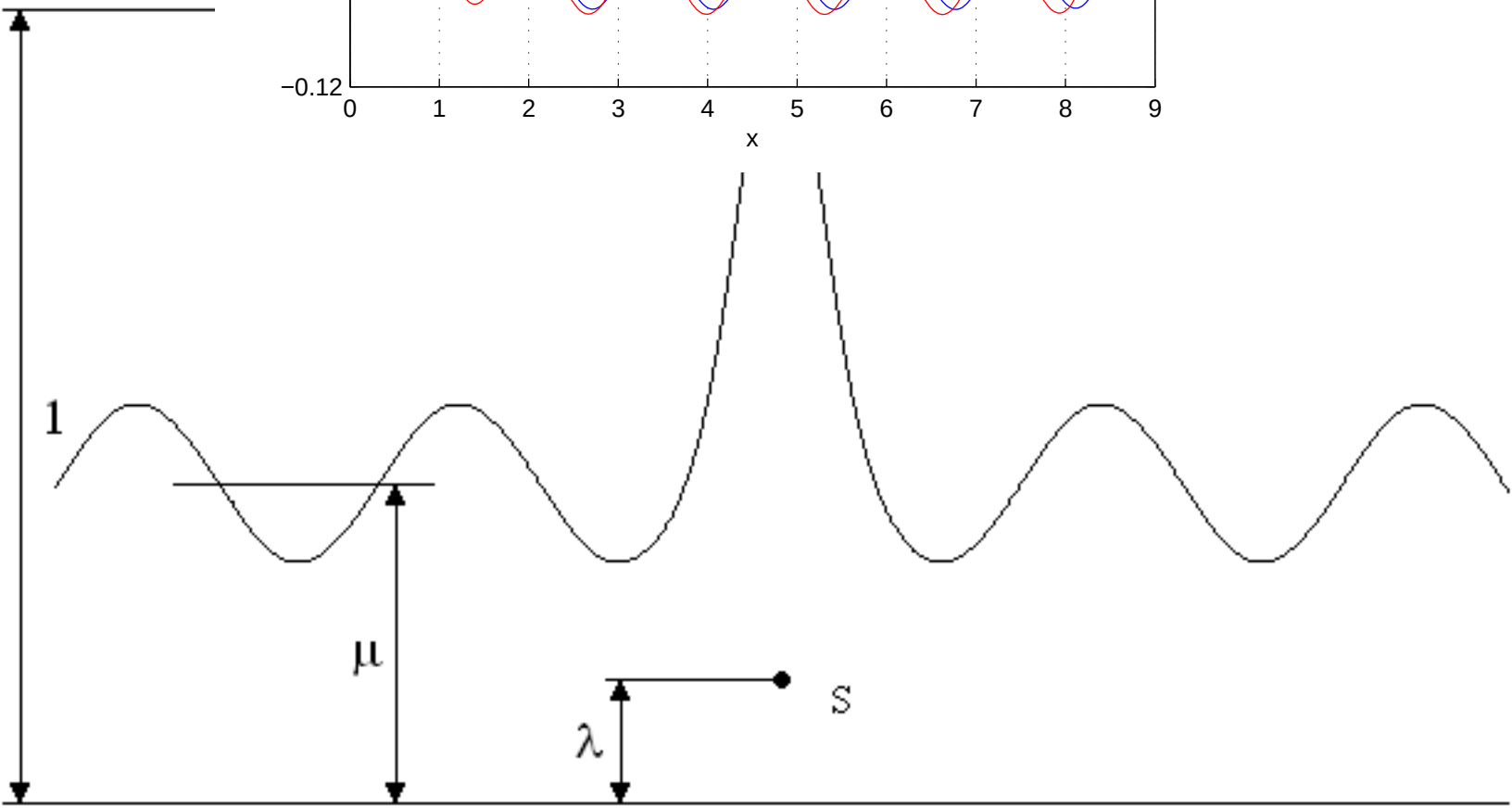
1
μ
λ
S

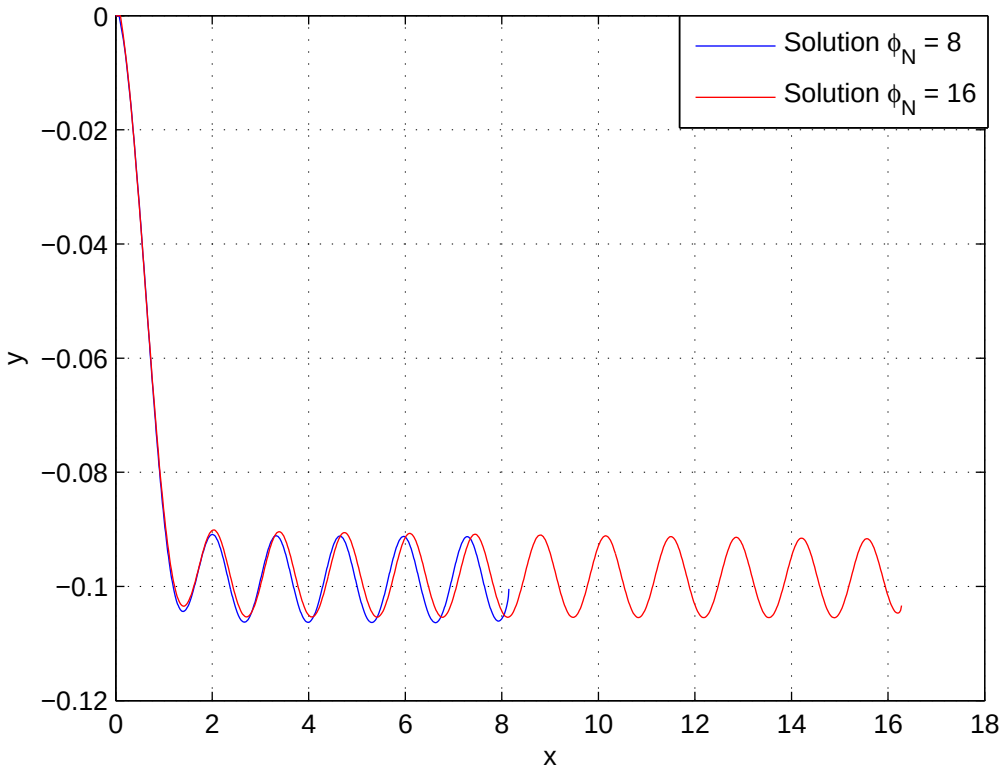
Solution $\phi_N$ = 8
Solution $\phi_N$ = 16
0
−0.02
−0.04
−0.06
−0.08
−0.1
−0.12
y
0
2
4
6
8
10
12
14
16
18
x